UNIVERSITY OF MINNESOTA
ST. ANTHONY FALLS HYDRAULIC LABORATORY

Project Report No. 242

COMPUTER SIMULATED MIGRATION OF MEANDERING RIVERS IN MINNESOTA

by

Helgi Johannesson

and

Gary Parker

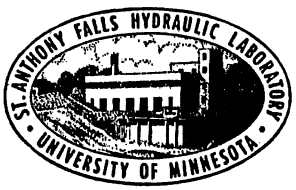

Prepared for

LEGISLATIVE COMMISSION ON MINNESOTA RESOURCES
State of Minnesota

September, 1985

Minneapolis, Minnesota

University of Minnesota
St. Anthony Falls Hydraulic Laboratory
Mississippi River at 3rd Ave. S.E.
Minneapolis, Minnesota 55414

Project Report No. 242

COMPUTER SIMULATED MIGRATION OF MEANDERING RIVERS IN MINNESOTA

by

Helgi Johannesson

and

Gary Parker

Prepared for

LEGISLATIVE COMMISSION ON MINNESOTA RESOURCES
State of Minnesota

September, 1985

ABSTRACT

In the present work, a computer model for simulation of the migration of meandering rivers, developed by Beck [1985a], was applied to four rivers in the State of Minnesota. The computer model is based on a theoretical approach developed by Ikeda, Parker, and Sawai [1981]. The major objective was to evaluate the overall performance of the computer model and to estimate the rates of river migration in Minnesota.

By using the model to analysis the past history of the four rivers, it was found that the model is able to reproduce the past river migration but needs considerable calibration. In all the case studies it was necessary to increase the dimensionless friction factor, C_f , considerably.

In all the study areas the rivers flow alternately through forested and non-forested areas. It was found that the rivers typically eroded about two times faster through non-forested areas than through forested areas. This result is of some interest, especially in agricultural areas. It indicates the importance of having a grove of trees lining the river instead of farming all the way to the river bank.

TABLE OF CONTENTS

Page

LIST OF FIGURES

LIST OF TABLES

LIST OF VARIABLES

A	transverse bed slope parameter.
A_g	drainage area for gaged site.
A_u	drainage area for ungaged site.
ARCD(I)	distance along the channel centerline to point No. I.
B	normal channel width.
B_o	normal channel width for a straight channel, $S_i = 1$.
$C = bC'$	dimensionless perturbation of $\tilde{C}$.
$\tilde{C}$	curvature.
C'	perturbation of $\tilde{C}$.
C_f	dimensionless Chezy friction factor.
$C_f^* = \frac{b}{H_o} C_f$	in Chapter II.
$C_{f1}^* = \frac{b}{H} C_f$	in Chapter II.
CVD(I)	value of $\tilde{C}$ for point No. I on the channel centerline.
D	mean particle diameter.
D_1	maximum local distortion in each aerial photograph.
D_2	estimated error in the location of the channel centerline due to the distortion in the aerial photographs.
E	erosion coefficient.
E_o	erosion coefficient (first order estimate of E).
$F = \frac{U}{(gH)^{1/2}}$	Froude number.

$F_o = \frac{U_o}{(gH_o)^{1/2}}$ Froude number for a straight channel, $S_i = 1$.

$F_D = \frac{U}{([(\rho_s-\rho)/\rho]gD)^{1/2}}$ particle Froude number.

H mean flow depth.

H_o mean flow depth for a straight channel, $S_i = 1$.

I water-surface slope.

I_o valley slope or water surface slope for a straight channel, $S_i = 1$.

L_o the valley length. Equals the length of a line following the river axis from the upstream end to the downstream end of the study reach.

Q flowrate.

Q_o flowrate for the straight channel, $S_i = 1$.

Q_b bankfull flowrate.

Q_g flowrate at the gaged site.

$Q_u = Q_g \left(\frac{A_u}{A_g}\right)^{0.6}$ flowrate at the ungaged site.

$S_i = \frac{I_o}{I}$ sinuosity of the river.

U mean velocity in the downstream direction.

U_o mean velocity in the downstream direction for a straight channel, $S_i = 1$.

XD(I) $\tilde{x}$ coordinate of point No. I on the channel centerline.

YD(I) $\tilde{y}$ coordinate of point No. I on the channel centerline.

$a_1 = \frac{k\, C^*_{f1}(A+F^2+1)}{k^2+4C^{*\,2}_{f1}}$ in Chapter II.

b the normal half-width of the channel.

$b_1 = \dfrac{2\, C^*_{f1}(A+F^2-1)-k^2}{k^2 + 4C^{*\,2}_{f1}}$ in Chapter II.

$e = \dfrac{1}{E_o}\dfrac{dE}{d\chi}$ in Chapter II.

g acceleration due to gravity.

$\tilde{h}$ flow depth.

h' perturbation of $\tilde{h}$.

h'_b value of h' at $\tilde{n} = b$.

$k = b\tilde{k}$ dimensionless wavenumber (Chapter II).

$\tilde{k} = \dfrac{2\pi}{\tilde{\lambda}}$ wavenumber (Chapter II).

$n = \dfrac{\tilde{n}}{b}$ dimensionless cross-stream coordinate.

$\tilde{n}$ cross-stream coordinate.

q_w water discharge per unit width of the channel.

$\tilde{r}$ radius of curvature.

$\tilde{r}_o$ minimum radius of curvature.

$s = \dfrac{\tilde{s}}{b}$ dimensionless downstream coordinate.

$\tilde{s}$ downstream coordinate.

$\tilde{t}$ time.

$\Delta\tilde{t}$ time step.

$u = \dfrac{u'_b}{U_o}$ dimensionless perturbation of $\tilde{u}$ at $\tilde{n} = b$.

$u_1 = \dfrac{u'_b}{U}$ dimensionless perturbation of $\tilde{u}$ at $\tilde{n} = b$.

$\tilde{u}$ velocity component in the downstream direction.

u' perturbation of $\tilde{u}$.

u'_b value of u' at $\tilde{n} = b$.

u_{ne} solution for u_1 for the case of neutral stability for a sine-generated curve.

$\tilde{v}$	velocity component in the cross-stream direction.
v'	perturbation of $\tilde{v}$.
$\tilde{x}$	coordinate in the Cartesian coordinate system used.
$\tilde{y}$	coordinate in the Cartesian coordinate system used.

Greek Symbols

α	the shift of the solution for u_1 relative to the solution for the case of neutral stability.
β	calibration coefficient in a possibly improved bank erosion model proposed in Chapter IV.
$\tilde{\zeta}$	bank erosion rate.
$\tilde{\eta}$	bed elevation.
η'	perturbation of $\tilde{\eta}$.
η_r	reference elevation for the bed.
θ	angle between the downchannel direction and the $\tilde{x}$-axis.
θ_o	value of θ for a sine-generated curve as the channel centerline crosses the downvalley axis.
$\theta(I)$	value of θ for point No. I on the channel centerline.
$\tilde{\lambda}$	meander wavelength measured along the channel centerline.
$\nu = \frac{b}{\tilde{r}_o}$	expansion parameter.
$\tilde{\xi}$	water-surface elevation.
ξ'	perturbation of $\tilde{\xi}$.
ξ_r	reference elevation for the water surface.
ρ, ρ_s	densities of water and sediment.
$\tilde{\tau}_s$	bed shear stress component in the downstream direction.
$\tilde{\tau}_n$	bed shear stress component in the cross-stream direction.
$\chi = (S_i)^{-1/3}$	in Chapter II.

I. INTRODUCTION

Natural, alluvial river channels can be divided into three catagories. They are either straight, meandering or braided. The work presented herein deals with the possibility of predicting the lateral migration of meandering rivers.

There are several reasons why being able to predict the future location of a river channel may be of importance. For example, when selecting a bridge site or a location of a road, it may be valuable to know the future impact of a nearby river on those structures. Secondly, when protecting existing structures from a migrating river by bank protection or other methods, it is necessary to have some means of knowing the response of the river to different engineering solutions. Thirdly, a migrating river may be eroding into valuable farmland, and having some means of estimating at which rate this is happening is of considerable interest.

Several people have tried to explain why rivers meander at all, and for a given meandering pattern have tried to predict the future location of the river. Since the original work of Hansen [1967] and Callander [1969] instability of the alternate bar type in straight channels has long been identified as the cause of fluvial meandering. The work of Hansen and Callander has been improved and extended by Adachi [1967], Hayashi [1970], Sukegawa [1970], Engelund & Skowgaard [1973], Parker [1975, 76], Ponce & Mahmood [1976], Hayashi & Ozaki [1976] and Fredsoe [1978]. All the above analyses are, however, unsatisfactory due to the fact that bank deformation is not allowed. By relaxing the restraint of fixed sidewalls, Ikeda et al. [1981] investigated the stability of channels with sinuous erodible banks and found conditions for the lateral bend amplitude to grow. Two instability mechanisms have therefore been identified:

1) The bar instability mechanism found by Hansen [1967] and Callander [1969]. The location of alternate bars in a straight channel is arbitrary.

2) The bend instability mechanism found by Ikeda et al. [1981]. The location of point bars on the inside of each bend is determined by curvature.

Ikeda et al. [1981] showed that, in the case of alluvial meanders, the two mechanisms operate at similar characteristic wavelengths. This suggests that alternate bars develop into true bends such that each bend contains one alternate bar. Recently, Blondeaux & Seminara [1985] reexamined the problem tackled by Ikeda et al. [1981]. They found that the bend instability mechanism does not select the most unstable wavelength of the bar instability mechanism, but rather that which is closest to producing resonance for any given set of flow parameters.

As mentioned before, the final goal is to be able to predict the future location of a river, given its current position. Hickin & Nanson

[1975] suggested the existence of a relationship between the outward normal migration rate and the ratio of half-width, b, to centerline radius of curvature, $\tilde{r}$. Their data, determined from scroll bars, indicates that normal outward migration rate increases as $b/\tilde{r}$ increases, up to a limiting value of $b/\tilde{r}$ of about 1/6. For tighter bends, the migration rate declines. This functional relationship between the outward normal erosion rate and $b/\tilde{r}$ may give a good general indication of the typical migration rate for a given bend but cannot be true for each point in that bend.

The first theory that can be applied directly to a given meandering river to study evolution of bends is that put forward by Ikeda et al. [1981]. It is interesting to note that Howard [1983] came up with a very similar theory based on essentially heuristic grounds. The overall performance of a computer model based on the theory developed by Ikeda et al. [1981] is discussed in the subsequent chapters. This model has been used by Parker [1982] to analyze the Minnesota River in Minnesota, by Beck et al. [1983a] to analyze the Pembina River in Alberta, Canada and by Beck et al. [1983b] to analyze the Genesee River in New York.

II. DERIVATION OF MODELLING THEORY

A. Introduction

A complete model of river meandering must provide a solution for the rates of bank erosion for each point along the river channel. A natural assumption is that for a given channel location and geometry the flow field can be calculated without any knowledge of bank erosion processes. Assuming some functional relationship between bank erosion rates and the flow field, a new channel location can be obtained. In this chapter, a theory which allows for calculation of the flow field and bank erosion rates is derived.

B. Equation Describing the Flow Field

1. Derivation

The flow field model is based on the depth-averaged momentum equations in the $\tilde{s}$ and $\tilde{n}$ directions and the depth-averaged continuity equation. These equations can be written as

$$\frac{1}{1+\tilde{n}\tilde{C}}\,\tilde{u}\,\frac{\partial\tilde{u}}{\partial\tilde{s}} + \tilde{v}\,\frac{\partial\tilde{u}}{\partial\tilde{n}} + \frac{\tilde{C}}{1+\tilde{n}\tilde{C}}\,\tilde{u}\tilde{v} = \frac{-1}{1+\tilde{n}\tilde{C}}\,g\,\frac{\partial\tilde{\xi}}{\partial\tilde{s}} - \frac{\tilde{\tau}_s}{\rho\tilde{h}} \tag{1a}$$

$$\frac{1}{1+\tilde{n}\tilde{C}}\,\tilde{u}\,\frac{\partial\tilde{v}}{\partial\tilde{s}} + \tilde{v}\,\frac{\partial\tilde{v}}{\partial\tilde{n}} - \frac{\tilde{C}}{1+\tilde{n}\tilde{C}}\,\tilde{u}^2 = -\,g\,\frac{\partial\tilde{\xi}}{\partial\tilde{n}} - \frac{\tilde{\tau}_n}{\rho\tilde{h}} \tag{1b}$$

$$\frac{1}{1+\tilde{n}\tilde{C}}\,\frac{\partial(\tilde{h}\tilde{u})}{\partial\tilde{s}} + \frac{\partial(\tilde{h}\tilde{v})}{\partial\tilde{n}} + \frac{C}{1+\tilde{n}\tilde{C}}\,\tilde{h}\tilde{v} = 0 \tag{1c}$$

where $\tilde{u}$ and $\tilde{v}$ are the depth-averaged velocity components in the $\tilde{s}$ and $\tilde{n}$ directions, g is the acceleration due to gravity, ξ is the water-surface elevation, $\tilde{\tau}_s$ and $\tilde{\tau}_n$ are the bed shear stress components in the $\tilde{s}$ and $\tilde{n}$ directions, ρ is the density of water, $\tilde{h}$ is the flow depth, and $\tilde{C}$ is the channel curvature along the centerline. Most of the above variables are shown in Fig. II.1. The tilde is used to denote dimensional variables.

The curvature is by definition equal to

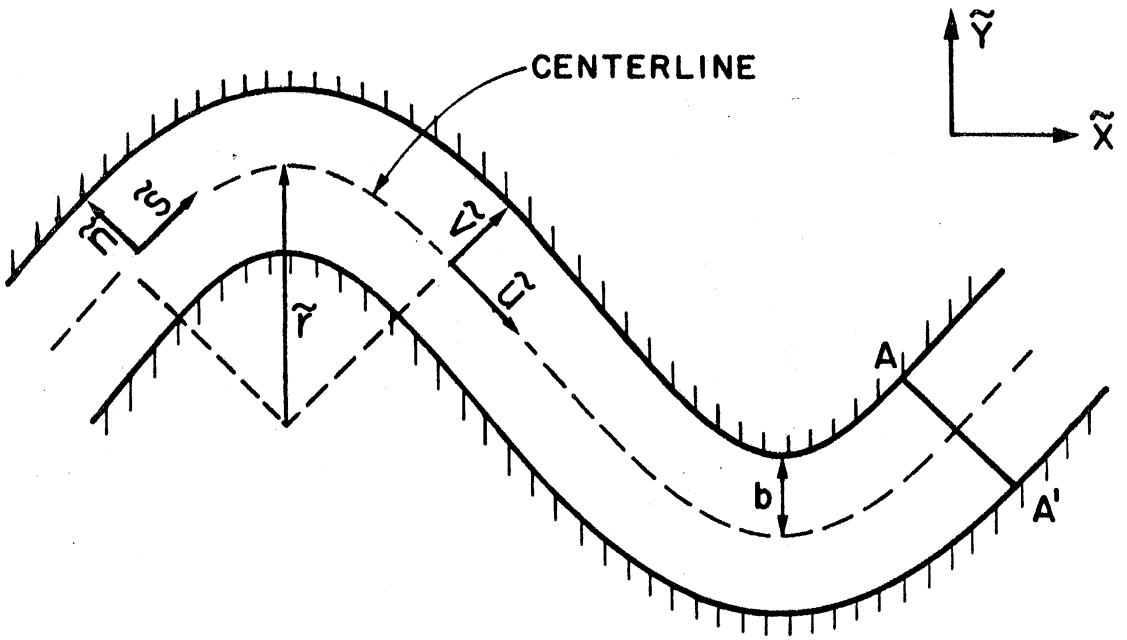

A) PLAN VIEW

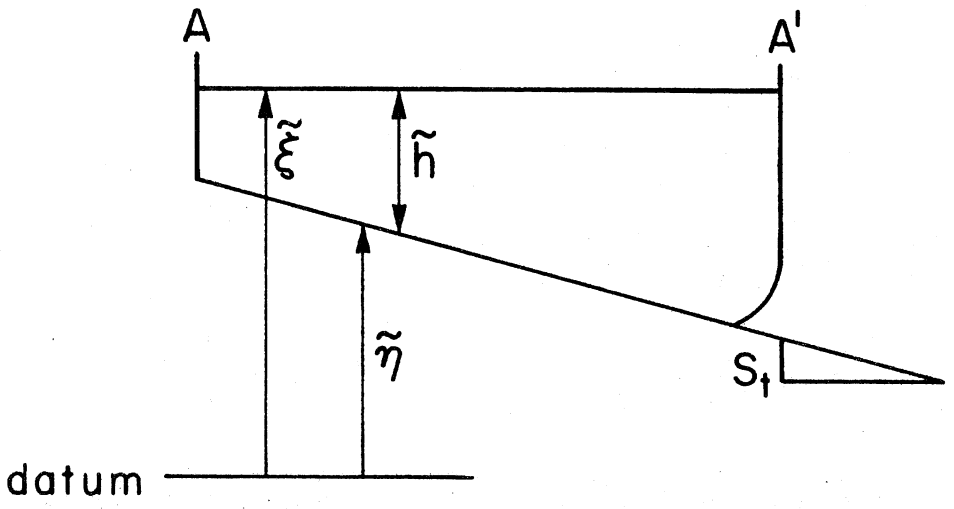

B) CROSS-SECTION A-A'

Fig. II.1. Definition of variables and coordinate system.

$$\tilde{C}(\tilde{s}) = -\frac{d\theta}{d\tilde{s}} = \frac{1}{\tilde{r}} \tag{2}$$

where θ is the angle between the downchannel direction and the $\tilde{x}$-axis.

Bed stresses are evaluated with the use of a friction factor, C_f;

$$\tilde{\tau}_s = \rho C_f \sqrt{\tilde{u}^2+\tilde{v}^2}\ \tilde{u} \tag{3a}$$

$$\tilde{\tau}_n = \rho C_f \sqrt{\tilde{u}^2+\tilde{v}^2}\ \tilde{v} \tag{3b}$$

Before proceeding further, the following assumptions are made:

1) Normal channel width is constant. This is suggested by the observation that many alluvial streams maintain roughly constant width even while actively migrating.

2) $\nu = b/\tilde{r}_o \ll 1$
where b is the normal half-width of the channel and $\tilde{r}_o$ is the minimum radius of curvature.

3) The meander wavelength $\tilde{\lambda} \gg b$

4) The flow is quasi-stationary, i.e. the time needed for the flow to adapt to a change in the bed level is much smaller than the time needed for the bed level change itself.

5) The friction factor, C_f , is constant.

Having made these assumptions, an informal perturbation expansion in ν up to $O(\nu^2)$ is carried out. Variables are written in terms of mean values plus a primed quantity denoting a perturbation induced by the channel curvature; $\tilde{u} = U+u'$, $\tilde{v} = 0+v'$, $\tilde{h} = H+h'$, $\tilde{\xi} = \xi_r - I\tilde{s}+\xi'$, $\tilde{\eta} = \eta_r - I\tilde{s}+\eta'$ and $\tilde{C} = 0+C'$. Here U is the mean tangential velocity, H is the mean depth, I is the average downchannel energy slope, and ξ_r and η_r are reference elevations for which $H = \xi_r - \eta_r$.

For zeroth order, Eqs. (1a) and (1c) give

$$C_f U^2 = g\ H\ I \tag{4a}$$

$$UH = q_w \tag{4b}$$

where q_w is constant water discharge per unit width. Equation (1b) does not contribute at zeroth order.

At $O(\nu)$, Eqs. (1a) and (1c) do not contribute and Eq. (1b) gives

$$U^2 C' = g \frac{\partial \xi'}{\partial \tilde{n}} \tag{5}$$

Equation (1b) does not contribute at $O(\nu^2)$ but Eqs. (1a) and (1c) give

$$U \frac{\partial u'}{\partial \tilde{s}} = - g \frac{\partial \xi'}{\partial \tilde{s}} - gIC'\tilde{n} - C_f \frac{U^2}{H} \left(\frac{2u'}{U} - \frac{\xi'}{H} + \frac{\eta'}{H} \right) \tag{6a}$$

$$H \left(\frac{\partial u'}{\partial \tilde{s}} + \frac{\partial v'}{\partial \tilde{n}} \right) + U \frac{\partial h'}{\partial \tilde{s}} = 0 \tag{6b}$$

The reach-averaged values for U, H and I are taken to be spatially constant but must vary slowly with time. If I_o is the valley slope, the sinuosity of the meandering channel is defined as

$$S_i = \frac{I_o}{I} \tag{7}$$

If the reach-averaged values of U, H and I for the straight channel, $S_i = 1$, are U_o, H_o and I_o, Eqs. (4a) and (4b) give the following result

$$U = U_o \chi(\tilde{t}) \tag{8}$$

$$H = \frac{H_o}{\chi(\tilde{t})} \tag{9}$$

$$\chi(\tilde{t}) = (S_i)^{-1/3} \tag{10}$$

Integration of Eq. (5) gives

$$\xi' = \frac{1}{g} C' U^2 \tilde{n} \tag{11}$$

To proceed further, a relation is needed for η'. Engelund [1974], Ikeda [1975], Kikkawa et al. [1976], Zimmerman & Kennedy [1978], and Odgaard [1981] have analyzed three dimensional flow in bends so as to account for secondary currents. Their result to $O(\nu)$ is

$$\frac{\eta'}{H} = - A\, C'\, \tilde{n} \tag{12}$$

Here the value of A is assumed to be constant. Appropriate values to use for A will be discussed later.

Substituting Eqs. (11) and (12) into Eq. (6a) and evaluating at $\tilde{n} = b$ gives

$$U \frac{\partial u'_b}{\partial \tilde{s}} + 2 \frac{U}{H} C_f u'_b = b \left[- U^2 \frac{\partial C'}{\partial \tilde{s}} + C_f C' \left(\frac{U^4}{gH^2} + (A-1) \frac{U^2}{H} \right] \right. \tag{13}$$

where $u'_b = u'$ at $\tilde{n} = b$. A dimensionless form of Eq. (13) is

$$\frac{\partial u}{\partial s} + 2\chi C_f^* u = \left[- \chi \frac{\partial C}{\partial s} + C_f^* C\left(F_o^2 \chi^5 + (A-1)\chi^2\right) \right] \tag{14}$$

where $u = u'_b/U_o$, $C = bC'$, $s = \tilde{s}/b$, $n = \tilde{n}/b$, $C^*_f = (b/H_o)C_f$ and $F_o = U_o/(gH_o)^{1/2}$.

Equation (14) is a nonhomogeneous, linear ordinary differential equation. Its solution is

$$\begin{aligned} u = {} & \left[u(0) + \chi C(0)\right] \exp\left(-2\chi\, C_f^*\, s\right) - \chi\, C(s) \\ & + C_f^* \left[\chi^2 (A+1) + F_o^2\, \chi^5\right] \exp\left(-2\chi\, C_f^*\, s\right) \int_o^s C(s') \exp\left(2\chi C_f^*\, s'\right) ds' \end{aligned} \tag{15}$$

It can be seen from Eq. (15) that the velocity perturbation, u, is influenced by three terms:

1) The upstream boundary values, u(0) and C(0), the influence of which decays exponentially in the downstream direction.

2) The local curvature, C(s).

3) The integrated effect of curvature, the influence of which decreases exponentially in the upstream direction.

2. Discussion

The derivation completed in the previous chapter differs slightly from the derivation performed by Ikeda et al. [1981]. They did not include the influence of the variation of curvature across the channel, and thus assumed that the radius of curvature at an arbitrary point in a bend is the same as that at the centerline. The variation of curvature across the

channel is taken into account herein by including the term $1/(1+\tilde{n}\tilde{C})$ in Eqs. (1a,b,c). This term should be included since in Eq. (1a) it introduces a new term of $O(\nu^2)$, as independently observed by Tamai et al. [1984]. Expanding the gravity term in Eq. (1a) gives

$$-\frac{1}{1+\tilde{n}\tilde{C}}\, g\, \frac{\partial \tilde{\xi}}{\partial \tilde{s}} \approx -(1-\tilde{n}C')g(-I + \frac{\partial \xi'}{\partial \tilde{s}})$$

$$\approx gI - g\frac{\partial \xi'}{\partial \tilde{s}} - \tilde{n}\, C'g\, I$$

where $-\tilde{n}C'gI$ is the additional term of $O(\nu^2)$. Due to this difference, the analysis of Ikeda et al. [1981] can be corrected by replacing A by A-1 therein.

Since this new term is equivalent to a simple modification of the value of A, it does not change the character of the solution. Nevertheless, this new term has considerable physical importance, as can be seen from the solution for a channel represented by a sine-generated curve.

If θ is the angle between the channel centerline and a line parallel to the downvalley direction, then a sine-generated curve is represented by the equation

$$\theta = \theta_o \cos(ks) \tag{16}$$

where k is a dimensionless wavenumber given by $k = b\tilde{k}$, $\tilde{k} = 2\pi/\tilde{\lambda}$, $\tilde{\lambda}$ is the meander wavelength measured along the centerline of the channel, and θ_o is the value of θ as the channel centerline crosses the downvalley axis (see Fig. II.2 for further explanation). Making variables dimensionless with U, H, and b instead of U_o, H_o, and b the solution of Eq. (15) can be written as

$$u_1 = k\theta_o \left(-a_1 \cos(ks) + b_1 \sin(ks)\right) \tag{17}$$

where

$$a_1 = \frac{k\, C^*_{f1}\, (A+F^2+1)}{k^2 + 4C^{*\,2}_{f1}} \tag{18a}$$

$$b_1 = \frac{2\, C^{*2}_{f1}\, (A+F^2-1)-k^2}{k^2 + 4C^{*2}_{f1}} \tag{18b}$$

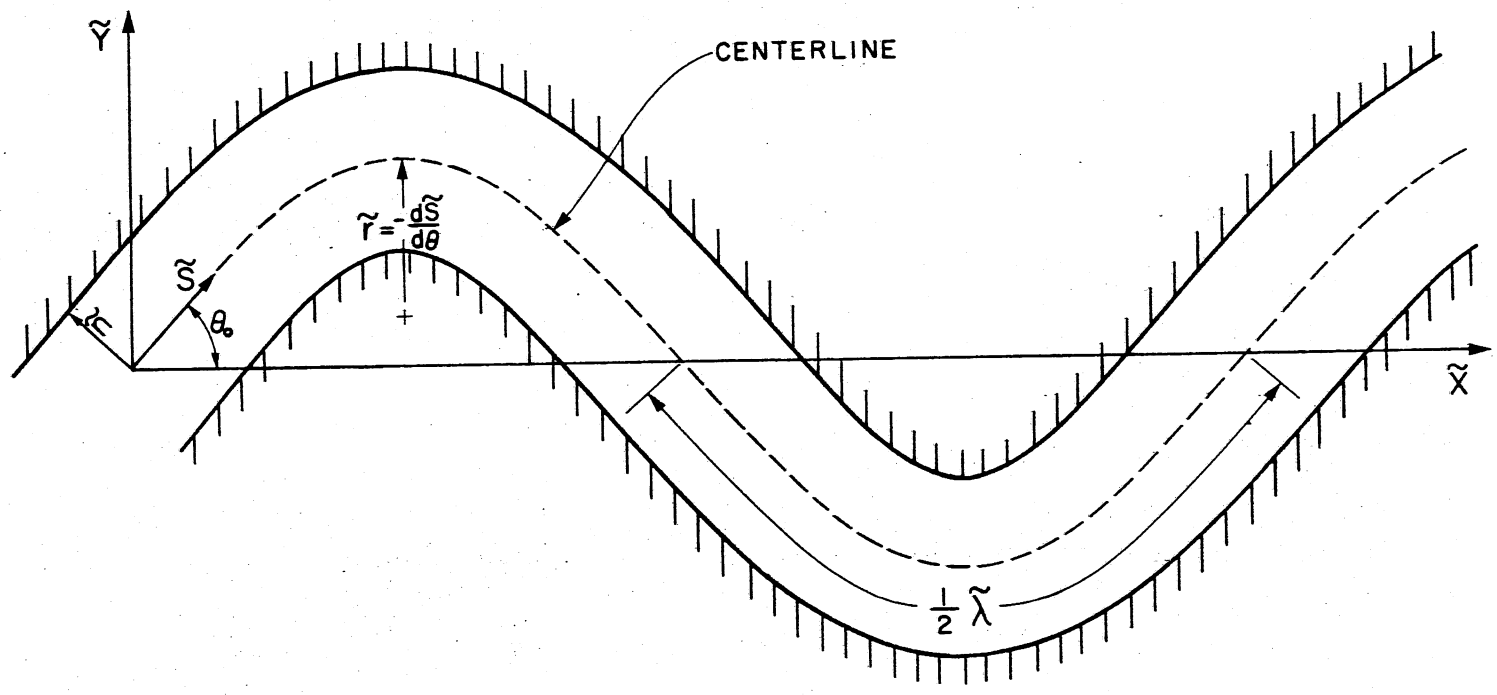

Fig. II.2. Definition diagram for the channel represented by a sine-generated curve.

Here $C^*_{f_1} = (b/H)C_f$ and $u_1 = u'_b/U$ since U and H are used instead of U_o and H_o to make variables dimensionless. Note that a_1 is always positive.

This solution is obtained under periodic equilibrium conditions, which means that the upstream boundary condition is neglected. In Section II.C.1, where the bank erosion equation is derived, it is assumed that the normal erosion rate of the left bank is a function of the tangential flow velocity near that bank. Assuming that bends grow in amplitude if the tangential flow velocity is higher at the outside bank than the inside bank at the bend apex and using Eq. (17), the implication is that bends grow in amplitude if $b_1 > 0$. This is exactly valid for small amplitude bends but only approximately valid for high amplitude bends. The following approximate condition for bend growth is therefore obtained

$$k < \sqrt{2}\, C^*_{f1}(A-1+F^2)^{1/2} \tag{19}$$

Equation (19) indicates that for a flat bed channel, i.e. $A = 0$, bends will not grow in amplitude unless the flow is supercritical, i.e. $F > 1$. This is an interesting condition which differs from the result obtained by Ikeda et al. [1981] that a flat bed channel could be unstable for certain combinations of $C^*_{f_1}$ and F even when the flow is not supercritical.

C. Equation Describing the Bank Erosion

1. Derivation

Ikeda et al. [1981] assumed that the normal bank erosion rate, $\tilde{\zeta}$, of the left bank is a function of the tangential flow velocity near that bank (Fig. II.3b). This functional relationship is estimated as

$$\tilde{\zeta} = \tilde{\zeta}(U) + \left.\frac{d\tilde{\zeta}}{d\tilde{u}}\right|_U u'(\tilde{s},b) \tag{20}$$

Assuming the river to have constant width in time, $\tilde{\zeta}(U)$ vanishes. Defining a positive coefficient of bank erosion $E(U) = [d\tilde{\zeta}/d\tilde{u}]|_U$, Eq. (20) becomes

$$\tilde{\zeta} = E(U)u'(\tilde{s},b) \tag{21}$$

Since U is a function of $\chi(t)$, $E(U)$ can be written as $E(\chi)$. A Taylor expansion of E about $\chi = 1$ gives

$$E(\chi) = E_o\big(1+e(\chi-1)\big) \tag{22}$$

where $E_o = E(1)$. Assuming $e(\chi-1)$ to be of secondary importance the following result for ζ is obtained

$$\tilde{\zeta} = E_o u'(\tilde{s},b) \tag{23}$$

The erosion coefficient, E_o, is a measure of the erodibility of the bank material.

A new channel location can then be calculated using what may be called a "Hickin mapping", in honor of the work of Hickin [1974]. As seen in Fig. II.3a, the channel migration is accomplished by shifting each point on the channel centerline some distance normal to the downstream direction. The distance is determined by Eq. (23). Referring in Fig. II.3b to a point on the channel centerline that is located at Cartesian coordinates $\tilde{x}_o$ and $\tilde{y}_o$ at time $\tilde{t}_o$, its coordinates a short time $\Delta\tilde{t}$ later are given by

$$\tilde{x} = \tilde{x}_o - \tilde{\zeta}\,\Delta\tilde{t}\sin(\theta) \tag{24a}$$

$$\tilde{y} = \tilde{y}_o + \tilde{\zeta}\,\Delta\tilde{t}\cos(\theta) \tag{24b}$$

The condition of constant width assures that the right bank, left bank, and the centerline all move in the same way, so that the erosion model is complete.

2. Discussion

It is interesting to compare the migration model derived herein with the idea of Hickin & Nanson [1975] that the outward normal erosion rate is a function of the dimensionless local curvature, C, as expressed by Eq. (25).

$$\tilde{\zeta} = f(C, \text{other parameters}) \tag{25}$$

Although the migration model proposed herein indicates that there is a convolutional relationship between migration rate and curvature, as expressed in Eq. (15), the downstream part of a bend, from the apex to the downstream inflection point, tends to approach developed bend flow. For a developed bend flow the curvature is constant and Eq. (15) reduces to

$$u = \frac{1}{2} C[\chi(A-1)+F_o^2\,\chi^4] \tag{26}$$

Equation (23) then becomes

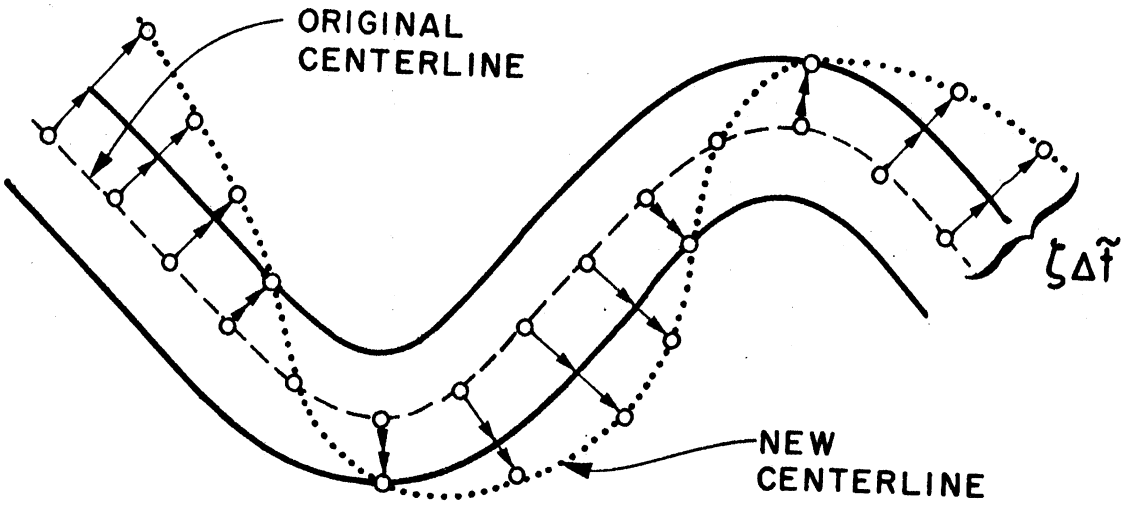

A) ILLUSTRATION OF THE USE OF THE ORTHOGONAL HICKIN MAPPING.

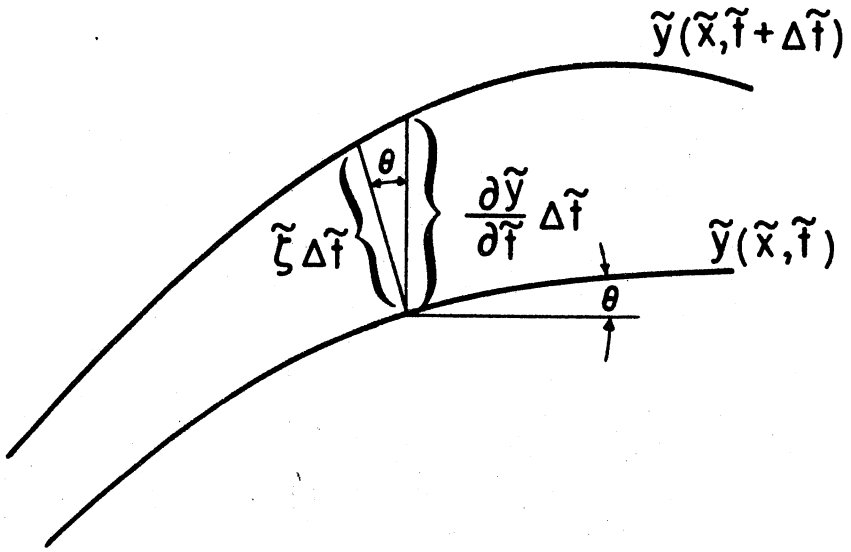

B) DIAGRAM FOR THE DERIVATION OF EQ. (2.24).

Fig. II.3. Definition diagram for the bank erosion model.

$$\tilde{\zeta} = \frac{1}{2} E_o U_o C[\chi(A-1)+F_o^2 \chi^4] \qquad (27)$$

and the migration rate is a function of the local curvature as suggested by Hickin & Nanson. Hickin & Nanson [1975] estimated the erosion rate from the relative age of scroll bars on the floodplain of the Beatton River, Canada. Since the migration is fastest in the downstream part of a bend, most of their data is in that region, which explains the similarity between Eqs. (25) and (27).

III. DESCRIPTION OF THE COMPUTER MODEL

Only a very short description is given of the computer model in this chapter. The version of the model used herein may differ slightly from a version of the same computer model used by Beck [1985a].

The equations to be solved are Eq. (15) for the velocity perturbation at the left bank at time $\tilde{t}_o$ and Eqs. (24a,b) for the new channel location at a short time $\Delta\tilde{t}$ later. Then knowing the initial location of the channel centerline, the location some years later is found by marching in time using $\Delta\tilde{t}$ as a time step.

The channel centerline, at time $\tilde{t} = \tilde{t}_o$, is characterized by discrete points with Cartesian coordinates $(\tilde{x},\tilde{y}) = (\tilde{x}_o(\tilde{s}),\tilde{y}_o(\tilde{s}))$. In order to solve Eq. (15) it is necessary to evaluate the curvature $\tilde{C}(\tilde{s})$ at each point. The curvature at any point is given by

$$\tilde{C}(\tilde{s}) = -\left(\frac{d\tilde{x}_o}{d\tilde{s}} \frac{d^2\tilde{y}_o}{d\tilde{s}^2} - \frac{d^2\tilde{x}_o}{d\tilde{s}^2} \frac{d\tilde{y}_o}{d\tilde{s}} \right) \tag{28}$$

A central differentiation scheme is used to solve for the curvature in Eq. (28). Having obtained the curvature for each point, Eq. (15) is easily solved numerically.

In order to solve Eqs. (24a,b) for the new channel location at time $\tilde{t} = \tilde{t}_o + \Delta\tilde{t}$, the angle, $\theta(I)$, must be calculated for each point I (see Fig. II.3 for the definition of θ). The angle, $\theta(I)$, is calculated as

$$\theta(I) = \arctan\left(\frac{YD(I+1) - YD(I-1)}{XD(I+1) - XD(I-1)} \right) \tag{29}$$

where XD(I) and YD(I) are the Cartesian coordinates of the Ith point. Having obtained the values of $\theta(I)$, Eqs. (24a,b) are easily solved with direct substitution of known values.

In order to get smooth initial values for the curvature, $\tilde{C}$, and the velocity pertubation, u', points that characterize the initial centerline location are eliminated so that if ARCD(I) is the distance along the channel centerline, from the upstream end to point No. I, then that point is eliminated if

$$[ARCD(I+1) - ARCD(I-1)] < 1.25B \tag{30}$$

where B is the channel width.

As the shape of the channel changes during the calculation, it is necessary to introduce new points by interpolation since the distance between any two points may become too large. It is also necessary to eliminate points if the curvature, CVD(I), at any point, I, becomes too large or if the distance between any two points becomes too small. The following criteria are used:

1) Point No. I is dropped if

$$|1.5/CVD(I)| < B \tag{31}$$

since the curvature is considered too large.

2) Point No. I is dropped if

$$[ARCD(I+1) - ARCD(I)] < 0.3B \tag{32}$$

since the distance between points No. I and I+1 is considered too small.

3) A point is added between points No. I and I+1 if all of the following conditions are satisfied:

a) $$[ARCD(I+1) - ARCD(I)] > 0.3B \tag{33a}$$

b) $$2[ARCD(I+1) - ARCD(I)]/[\,|1/CVD(I+1)|+|1/CVD(I)|\,] > 0.3 \tag{33b}$$

c) $$|1.3/CVD(I)| > B \tag{33c}$$

d) $$|1.3/CVD(I+1)| > B \tag{33d}$$

A parabolic regression with four datapoints, (points No. I-1,I,I+1,I+2), is used to interpolate new points. Conditions a) and b) ensure that a new point is interpolated if the distance between any two points is too large. Conditions c) and d) ensure that interpolation is not performed if the curvature is close to being too large at the neighboring points, since then the new point might have a curvature that is too high.

All the above-mentioned criteria are based on the experience gathered during the application of the model to actual rivers.

IV. MODEL APPLICATION

A. General Procedure

1. Selection of Study Areas

As mentioned before, the model was applied to four rivers in the State of Minnesota. The locations of the study areas are shown in Fig. IV.1. The selection of the study sites was based on five main criteria:

1) The river must have shown a considerable amount of migration within the study area during the period of record.

2) Aerial photographs, showing clearly the location of the river channel within the study area, should be available for at least three different years. This allows for both calibration and verification of the model.

3) The river must be gaged within or close to the study area.

4) Some cross-sectional measurements must be available within or close to the study area.

5) A topographical map showing the study area, preferably with a scale equal to or larger than 1:24000, should be available.

Having chosen a study area that satisfied the above-mentioned criteria, the topographical map was enlarged to a convenient scale. The aerial photographs were enlarged until they matched the topographical map as accurately as possible. The centerline of the river was then traced from the aerial photographs. Local distortion was partially accounted for as follows. Each of the aerial photographs was placed on the topographical map, and as the centerline was traced, the aerial photograph was moved a little in order to get as good a local fit as possible. Then the reach where the river had been most active was chosen for computer analysis. The length of the study reach varied between 3.5 to 7 km for these four rivers. The $\tilde{x}$ and $\tilde{y}$ coordinates of the channel centerline were read directly from a drawing into an Apple computer, using a data digitizer.

2. Estimation of Input Parameters

In addition to a knowledge of the initial location of the river channel, the following input parameters were required for the computer model:

1) The valley length, L_o

2) The average channel top-width, B_o

3) The average channel depth, H_o

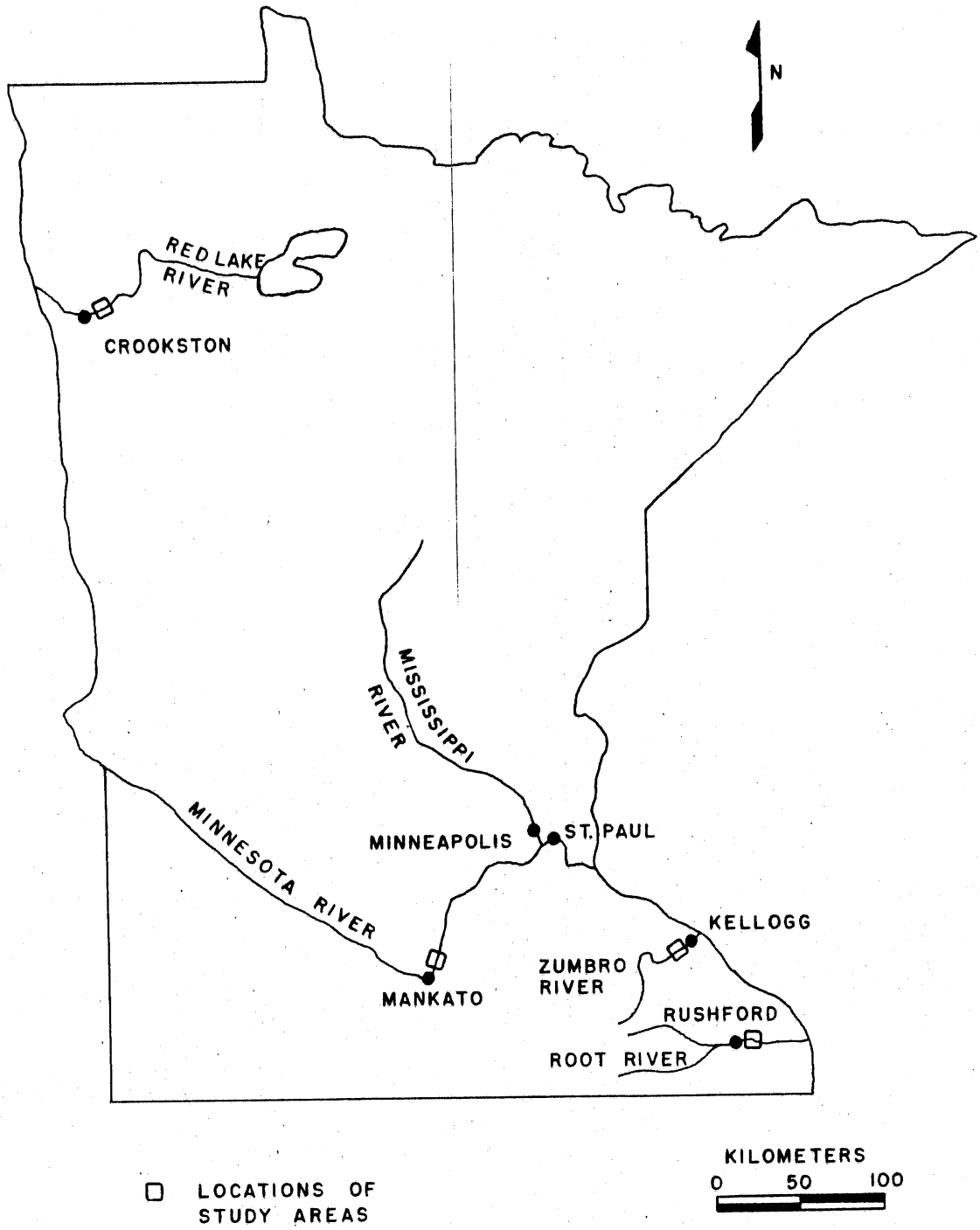

Fig. IV.1. Locations of the study areas.

4) The valley slope, I_o

5) The mean flow velocity, U_o

6) The Froude number, F_o

7) The dimensionless Chezy friction factor, C_f

8) The transverse bed slope parameter, A

9) The time increment, $\Delta\tilde{t}$

10) The value of the dimensionless left bank velocity at the upstream end, $u(0) = u'_b(0)/U_o$

11) The erosion coefficient, E_o

12) The locations of inerodible barriers or bank revetments

All of the above variables were estimated for the case of bankfull flow.

The valley length, L_o, is defined as the length of a line following the river axis from the upstream end to the downstream end of the study reach, as illustrated in Fig. IV.2.

The average channel top-width, B , and the average channel depth, H , were found from cross-sectional measurements. B_o and H_o are corresponding values that would result if the sinuosity of the river were equal to 1. The assumption of constant width gives $B_o = B$. Equation (9) was used to find H_o.

The water-surface slope, I, was found by plotting the longitudinal profile of the river, using the topographical map and information from the cross-sectional measurements. The valley slope, I_o , is the corresponding slope that would result if the sinuosity of the river were equal to 1. It was found by plotting the longitudinal profile of the river axis.

Although the model has means to account for the time-integrated effect of the entire range of flows that the river may be expected to have, it was assumed that the flow rate was constant and equal to the bankfull flow rate Q_b. This is a good assumption, even though bankfull flow occurs only for a small percentage of the time on most streams, since most of the erosion likely takes place when the flow is close to being bankfull. The bankfull flow was estimated by using the cross-sectional measurements, the previously-obtained longitudinal profile of the river, and a discharge rating curve for a nearby gage site. The average velocity for bankfull flow, U, was then calculated as $U = Q_b/BH$. U_o is the corresponding velocity that would result if the sinuosity of the river were equal to 1. Equation (8) was used to calculate U_o. Having obtained values for U_o and H_o , the Froude number, F_o , was calculated as $F_o = U_o/\sqrt{gH_o}$.

The dimensionless friction factor, C_f, was calculated from Eq. (4a). In order to get good agreement between the calculated and the observed channel locations, when the model was calibrated, it was necessary to use values of C_f determined from calibration that differed from the actual values.

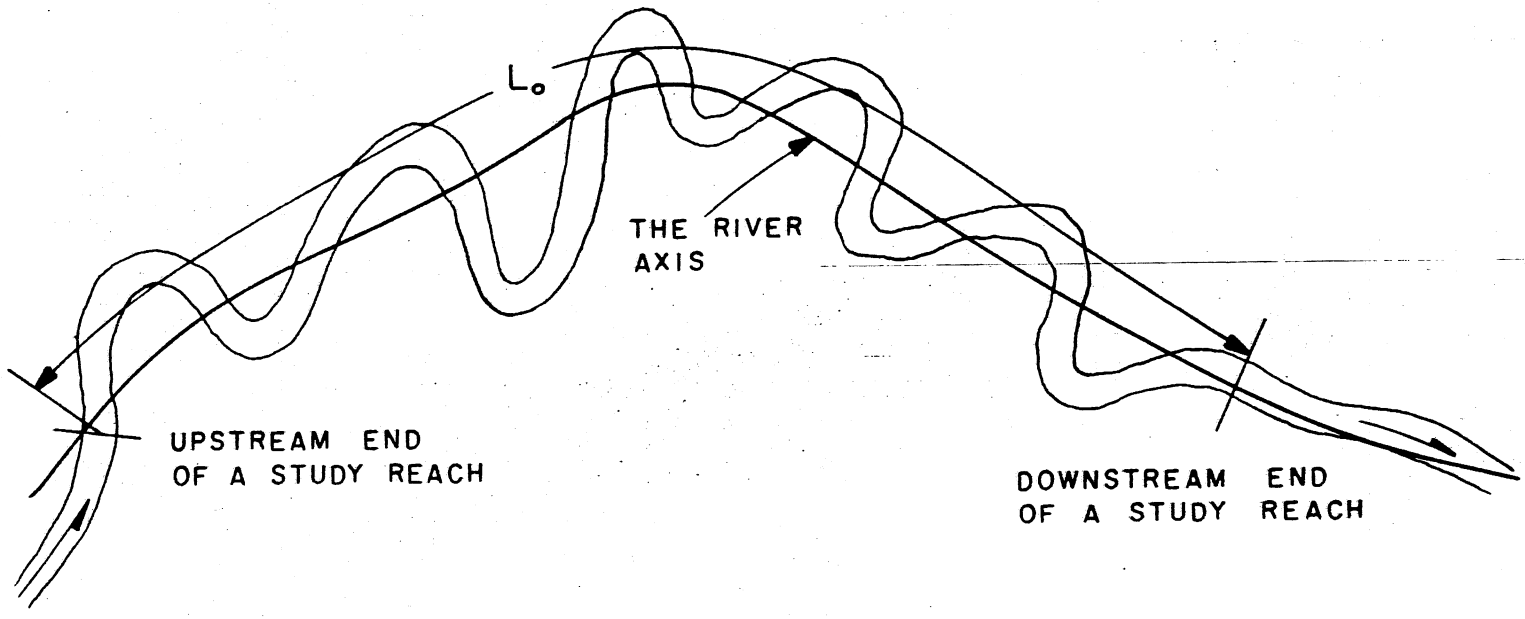

Fig. IV.2. Definition of the valley length, L_o .

It was assumed that the transverse bed slope parameter A was equal to six for all the four rivers. Originally, it was intended to calibrate the model by varying the value of A instead of C_f. This would have been the natural thing to do since C_f could be calculated, but the value of A could only be estimated if extensive cross-sectional measurements were available, which was not the case. However, the model proved to be more sensitive to the value of C_f than to the value of A. So instead of calibrating the model by changing both C_f and A, the value of A was kept constant.

Bed topography for fully developed flow in a channel with constant radius of curvature has been analyzed theoretically by Kikkawa et al. [1976], Zimmerman & Kennedy [1978] and Odgaard [1981]. All the models predict the result given by Eq. (12), although they differ slightly in the evaluation of A. These models indicate that A increases with increasing particle Froude number, $F_D = U/\left(\left[(\rho_s-\rho)/\rho\right]gD\right)^{1/2}$ where ρ is the density of water, ρ_s is the density of the sediment particles and D is the mean particle diameter. Zimmerman & Kennedy [1978] did several experiments and obtained average value of A equal to 4.3. Kikkawa et al. [1976] compared their theory with field data obtained by Rozovskii [1957] and estimated the value of A to be equal to eight. Engelund [1974] analyzed the case of sinuous, meandering channel and obtained Eq. (12) as a first order approximation for the bed topography. He suggested a constant value of A equal to four. Engelund carried his analysis to higher order and obtained a result which indicates that there is some lag distance between the bed topography and the channel curvature. It is assumed herein that this lag distance is small enough so that the bed topography can be represented by Eq. (12). Finally, it is worth mentioning that an analysis of 45 bends of ten alluvial rivers in Japan, based on data collected by Suga [1963], suggests an average value of A equal to 2.9, although the data show much scatter. Since the average values for A reported in the literature vary approximately from 3 to 8, the selection of the constant value of A to be equal to six seems appropriate.

The time increment, $\Delta\tilde{t}$, was selected to be equal to 0.25 years for all the computer runs. This was based on the fact that smaller time steps did not give significantly different results.

The value of the dimensionless velocity perturbation at the upstream end, u(0), had to be estimated since the velocity distribution at the upstream end was not necessarily uniform. If possible, the location of the upstream end for each study reach was selected at the downstream end of a rather straight reach. This led to an estimation for the value of u(0) of 0.0. This was the case for all the rivers except the Minnesota River.

Based on the aerial photographs, each study area was divided into forested and non-forested zones. One value of the erosion coefficient, E_o, was used to characterize all the forested zones and another value of E_o was used to characterize all the non-forested zones, as done by Beck et al. [1983b] when studying the Genesee River. Generally, the erosion coefficient can be assumed to be lower for forested areas than for non-forested areas. The values of E_o were changed during the calibration process until the best possible agreement was obtained between the calculated and the measured channel locations. When the size and the location of forested areas changed within the calibration or the verification period, the

locations of forested zones, to be used for the computer simulation, were based on the aerial photograph from the year when the simulation started.

Finally, the locations of inerodible barriers such as valley walls or bank revetments were specified. A routine in the computer program checks to see if any point on the channel centerline is moving through an inerodible barrier, and shifts it back if that is the case. Since the channel location was characterized by the channel centerline, locations of valley walls and bank revetments were shifted approximately half the channel width towards the centerline of the channel before being read directly from a drawing into an Apple computer, using a data digitizer.

3. Estimation of Errors in the Input Parameters

The largest error was probably introduced by the decision of keeping A constant, and equal to six, for all the rivers. The only way to reduce this error would have been to make extensive cross-sectional measurements within the study areas, preferably during rather high flows. Based on available data in the literature, the value of A could easily vary from about 2 - 10, indicating that the value of A, used herein, might possibly be somewhere between three times too high or 1.7 times too low for each of the rivers analyzed.

Available cross-sectional measurements were used to find average depth, H, and width, B. Maximum error in these parameters was estimated to be about 10-20%, depending on the amount and the locations of the measurements. This error is of the same order as the error introduced by the assumption that the river width is constant for the whole study reach.

The error in the valley slope, I_o , was estimated to be about 10%, which is less than the error introduced by assuming the river to have constant slope throughout the study reach.

The error in the bankfull flowrate was estimated to be of the order of 10 - 15%. The main source of this error was the fact that a river usually is less than bankfull at one location, although it is more than bankfull at some other location. This error did not influence the final result of the computer simulation very much since any error in the flow rate changes only the computed mean flow velocity, U, and the observed friction factor, C_f . Since the value of C_f was calibrated, this error only influenced the calibrated values of the erosion coefficient, E_o, as can be seen from Eqs. (23) and (24). However, due to the fact that the calibrated values of C_f are later compared to the observed values, it is important to know how accurately the observed values of C_f were calculated.

Having estimated the percentage errors in Q_b , B, H, and I, the estimated maximum error in the observed value of C_f is of the order of 140%. However, it is inappropriate to expect the error in any of the four calculated values of C_f to be this large, unless the errors become added in the most unfavorable way, which is rather unlikely.

Finally, errors were introduced into the calculation when the initial location of each channel centerline was determined from the aerial photographs. There were two reasons for this error:

1) The local distortion in the aerial photographs. The magnitude of this error was estimated for each aerial photograph and is listed in Table 1. It varies between 5 - 21% of the channel width, B, but is generally of the order of 10%.

2) When the channel centerline was traced from the aerial photographs, error was caused by the fact that the photographs in many cases were taken when the flow differed significantly. Secondly, in several locations the river banks were not steep and well defined. Therefore, subjective judgement influenced the result. The error in the initial location of the channel centerline due to this factor was estimated to be of the order of 10% of the channel width, B.

4. Model Calibration

As mentioned before, the model was calibrated by optimizing the values of E_o and C_f until the best possible agreement was obtained between the calculated and measured channel locations.

The value of E_o influences only the magnitude of the predicted river movement. It can be determined only by means of optimization and will generally depend upon the erosive resistance of the bank material.

The calibration of C_f allows for partial correction for:

1) Inaccuracies inherent in the basic equations.

2) Errors introduced by the selection of A = 6.

3) Errors in the calculation of the observed value of C_f.

The influence of changing C_f is more complicated than the influence of changing E_o, but can be qualitatively described by studying the case of a sinusoidal channel. Defining the channel shape by Eq. (16), the solution of Eq. (15) can be written as

$$u_1 = k\theta_o\left(-a_1\cos(ks) + b_1\sin(ks)\right) \tag{34}$$

Neutral stability occurs when $u_1 = 0$ at the bend apex. For that situation b_1 is equal to zero and $u_1 = u_{ne}$ where

$$u_{ne} = -k\theta_o a_1\cos(ks) \tag{35}$$

Equation (34) can also be written as

$$u_1 = -k\theta_o\sqrt{a_1^2 + b_1^2}\cos(ks+\alpha) \tag{36}$$

where $\alpha = \arctan(b_1/a_1)$ is the shift, upstream ($\alpha > 0$) and downstream ($\alpha < 0$), of the solution for u_1 relative to the solution for the case of

TABLE 1. ERROR IN CHANNEL CENTERLINE LOCATION DUE TO DISTORTION IN AERIAL PHOTOGRAPHS

River Name	Reach Location	Aerial Photograph From	D_1[f1] (m)	D_2[f2] (m)	D_2 (% of B)[f3]
Root River	Near Rushfield	1947	12	6	11
		1968	12	6	11
		1979	12	6	11
Zumbro River	Near Kellogg	1938	12	6	9
		1958	9	4.5	7
		1980	12	6	9
Minnesota River	Near Mankato	1938	11	5.5	5
		1961	11	5.5	5
		1980	11	5.5	5
Red Lake River	Near Crookston	1939	12	6	7
		1954	36	18	21
		1977	24	12	14

f1 D_1 is the maximum local distortion in each aerial photograph.

f2 D_2 is the estimated error in the location of the channel centerline due to the distortion. D_2 is less than D_1 since the channel centerline was traced from the aerial photographs in such a way that D_2 was minimized.

f3 B is the channel width.

neutral stability. The value of $\sqrt{a_1^2 + b_1^2}$ can be referred to as the amplitude of the solution. The values for α and $\sqrt{a_1^2 + b_1^2}$ are plotted as a function of k/C^*_{f1} in Fig. IV.3. For the construction of this graph a_1 and b_1 are calculated from Eqs. (18a,b), assuming that A = 6 and F = 0.0. It is reasonable to neglect the influence of F since F << A for the case where A = 6.

The influence of changing the value of C_f is illustrated in Fig. IV.3. As C_f is increased, α increases and the point of crossing of the thread of high velocity, from the inner to the outer bank, is shifted in the upstream direction, finally making the bend unstable at $k/C^*_{f1} = \sqrt{2(A-1)} = 3.16$. For the limiting case of $C^*_{f1} \to \infty$ α is equal to $\pi/2$ and the velocity perturbation, u_1, at either bank, follows the channel shape, having its maximum at the outside bank at a bend apex. Also, as C_f is increased, $\sqrt{a^2_1 + b^2_1}$ increases, as shown in Fig. IV.3b, indicating that the maximum value of the velocity perturbation, u_1, increases, leading to generally higher lateral migration rates unless E_o is decreased.

The nature of the influence of the calibration of the parameters, C_f and E_o, leads to a rather easy calibration procedure. The value of C_f is adjusted until a satisfactory migration pattern in obtained. The value of E_o is adjusted until satisfactory erosion rates are obtained.

B. Root River Case Study

1. The Hydraulic and Geomorphic Setting

The Root River, shown in Fig. IV.4, originates from the confluence of the Middle Branch Root River and the South Branch Root River, just east of Lanesboro. It flows in an easterly direction toward its confluence with the Mississippi River.

The reach chosen for the present computer analysis is located just east of Rushford. It is approximately 3.5 km long.

The river valley. On both sides of the valley, the terrain rises to about 120 m above the valley bottom. The valley has a bottom width of about 0.7 km and is filled with fine to medium sand.

Channel planform. From 1947 to 1979, the sinuosity of the river increased, from 1.6 to 1.8, in the study area. The river flows alternately through forested and non-forested areas. Throughout the period of record, the amount and location of non-forested areas along the river banks has changed. In 1947, non-forested areas were located along the river banks for about 23% of the length of the reach. In 1968 and 1979, the corresponding values were 53% and 37%.

In some areas, the lateral migration of the river has been or will be restricted by:

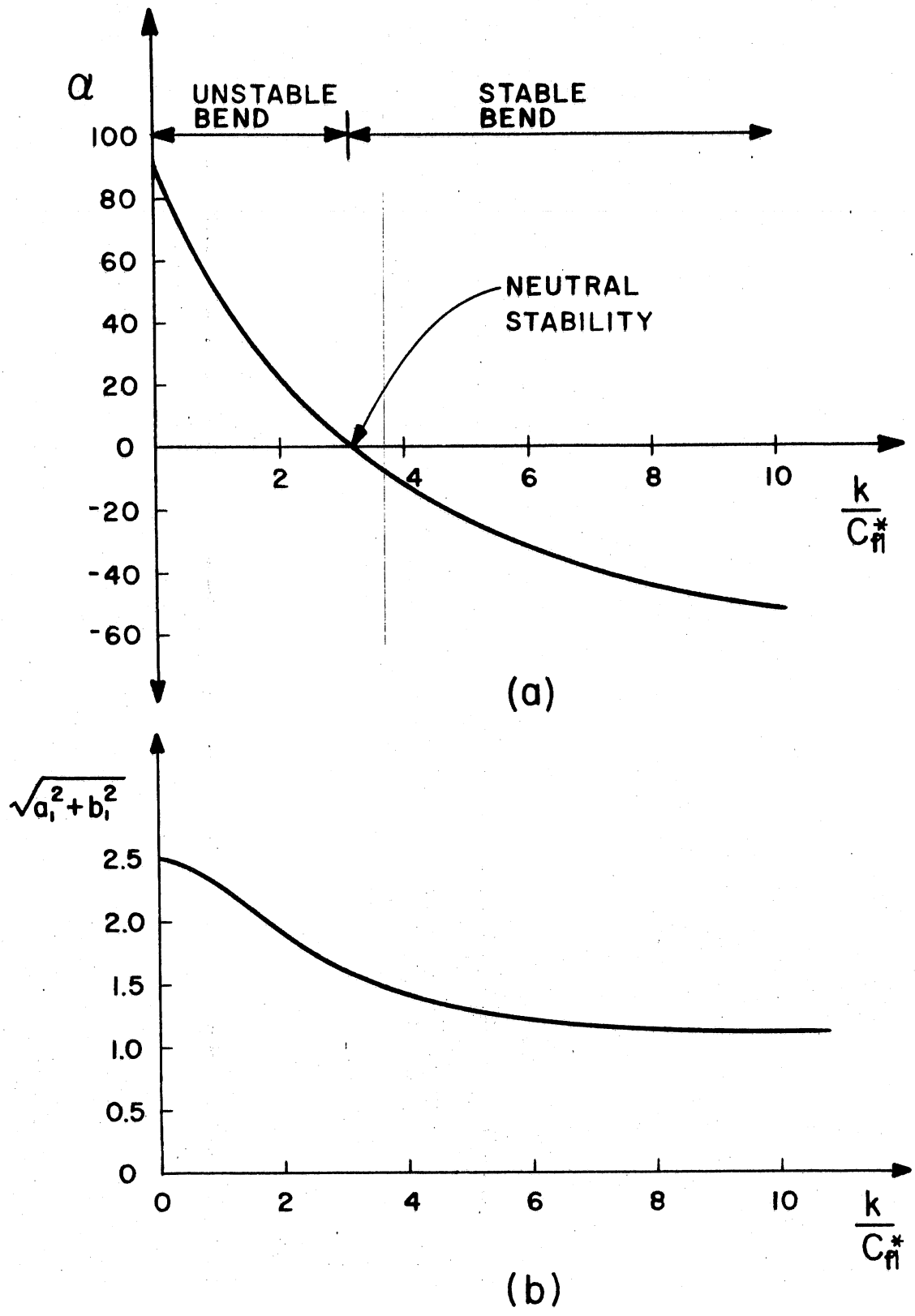

Fig. IV.3. a) the shift α and b) the amplitude $\sqrt{a_1^2 + b_1^2}$ as a function of k/C^*_{f1}.

1) Valley walls.

2) Existing bank protection along parts of an abandoned railroad, shown in Fig. IV.7. This railroad was constructed in 1870 and abandoned in 1979.

Hydrology. The Root River is not gaged within the length of the study reach. However, inferences as to hydrologic conditions could be made from the gaging station at Houston (Fig. IV.4). This gaging station has been in operation since 1930. The difference in discharge between the study reach and Houston was assumed to be negligible due to the lack of substantial tributaries in between. Data for various flood flows are listed in Table 2; the information was compiled by the U.S. Geological Survey.

A rating curve was obtained for the gage site at Houston. This, together with cross-section data obtained near the gaging station, allowed for an estimate of bankfull flow at Houston. Bankfull flow in the study reach is assumed to be the same as bankfull flow at Houston.

Channel geometry. Several cross-sections just upstream of the study reach were surveyed in 1963 by the St. Paul District of the U.S. Army Corps of Engineers. Locations of these cross-sections are shown in Fig. IV.5. Some typical cross-sections are shown in Fig. IV.6, and cross-section characteristics are listed in Table 3. These measurements, together with a topographical map, allowed for estimation of average bankfull geometry and flow parameters for the river reach between cross-sections No. 9 and 21, as shown in Table 4. This reach had a sinuosity equal to 1.55 in 1963. Bankfull geometry and flow parameters that would result if the river were straight, $S_i = 1$, were computed for the reach between cross-sections No. 9 and 21. They were assumed to be the same for the study reach. These parameters were used as input data in the program, and are listed in Table 4.

2. History of Channel Planform

Aerial photographs of the channel for the years 1940, 1947, 1962, 1968, 1979, and a topographical map based on aerial photographs from 1974 and 1975 were obtained. The topographical map and the aerial photographs from 1947, 1968, and 1979 were enlarged to a common scale. In Fig. IV.7, the 1947, 1968, and 1979 channels are shown. Upstream of the study reach, the movement of the river was partly due to manmade cutoffs. The rest of the river moved in a classical meandering pattern. Bends tended to erode in the outward direction and shift in the downstream direction. It can be seen how bank protection has restricted the movement of the river close to the railroad track.

3. Computer Analysis

The model was calibrated by optimizing the erosion coefficient, E_o, and the dimensionless friction factor, C_f. The period between 1968 and 1979 was used for the calibration, and the following values were obtained:

Non-forested areas $E_o = 1.1 \cdot 10^{-7}$

Forested areas $E_o = 6.0 \cdot 10^{-8}$

$C_f = 0.013$

TABLE 2. VARIOUS FLOOD FLOWS FOR THE ROOT RIVER

Flow	Discharge at Houston (m^3/s)
bankfull	430
2-year	310
5-year	520
10-year	670
25-year	860
50-year	1000
100-year	1130
largest on record	1050

TABLE 3. CROSS-SECTION CHARACTERISTICS

Cross-section Number	Top Width (m)	Mean Depth (m)
9	93	2.5
10	44	3.3
11	47	2.8
12	43	2.7
13	75	2.8
14	70	1.9 (Not typical)
15	51	2.9
16	46	2.7
17	62	2.7
18	53	3.0
19	44	2.8
20	58	3.0
21	44	3.5

Table 4. Average Parameters at Bankfull Flow

	River Channel	Straight Channel
Water surface slope	$I = 5.44 \cdot 10^{-4}$	$I_o = 8.43 \cdot 10^{-4}$
Channel width	$B = 55.1$ m	$B_o = 55.1$ m
Mean depth	$H = 2.90$ m	$H_o = 2.51$ m
Discharge	$Q = 430$ m^3/s	$Q_o = 430$ m^3/s
Mean flow velocity	$U = 2.71$ m/s	$U_o = 3.13$ m/s
Froude number	$F = 0.51$	$F_o = 0.63$

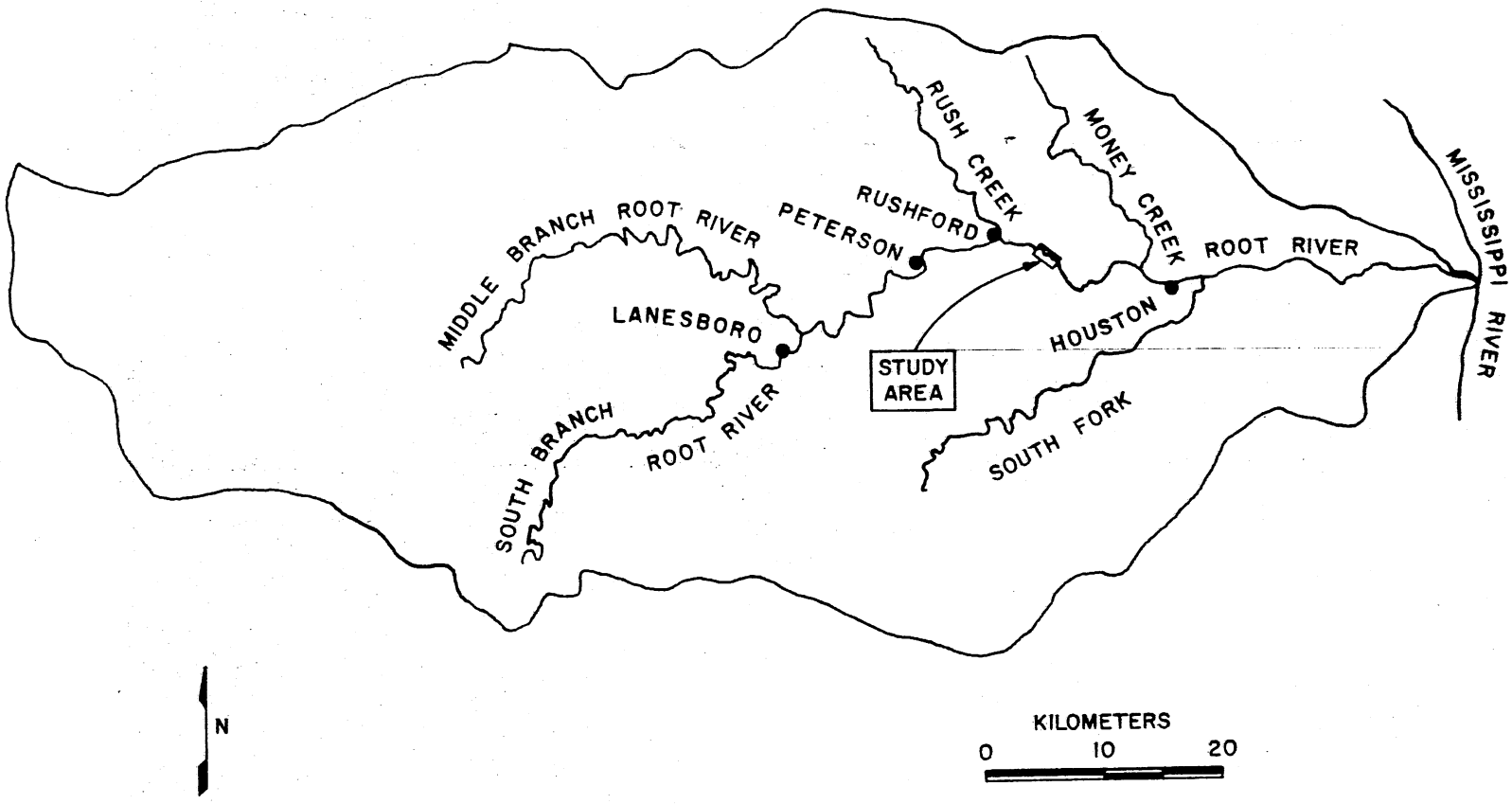

Fig. IV.4. The Root River watershed.

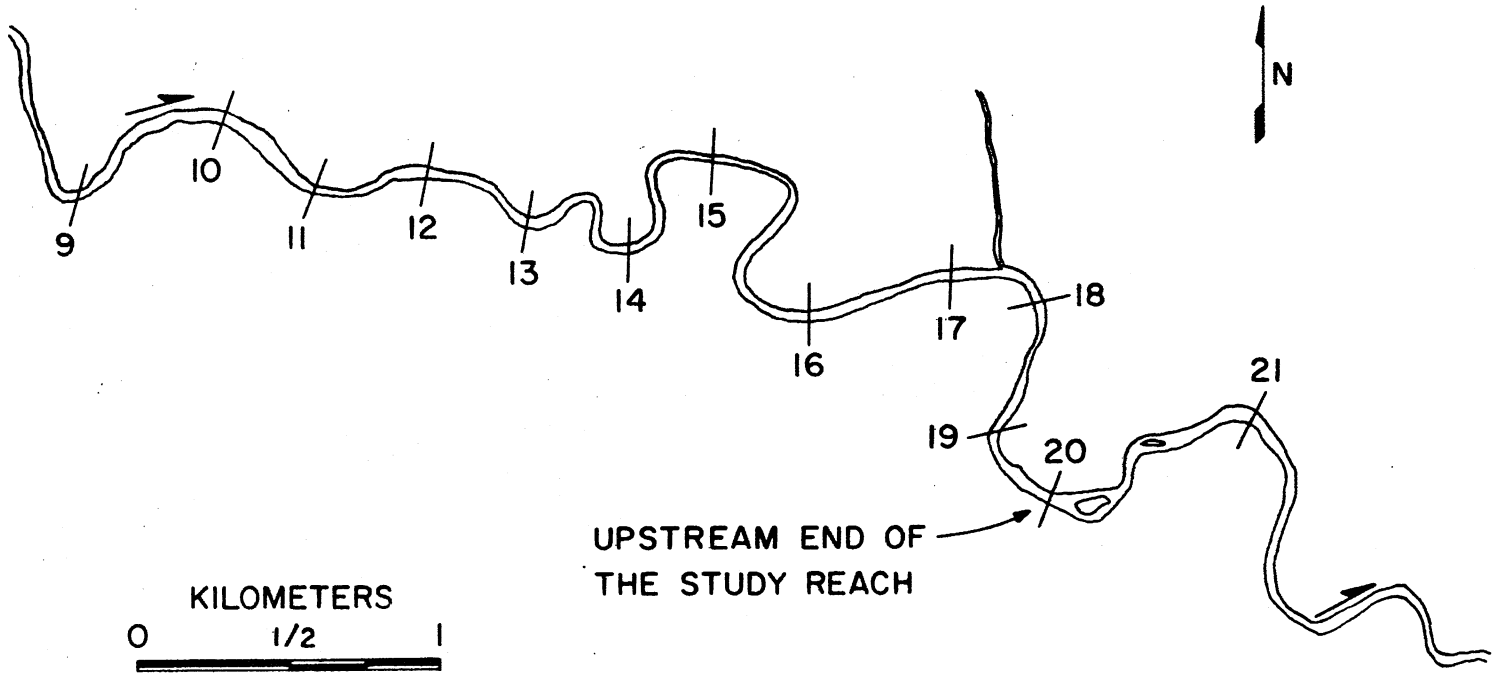

Fig. IV.5. Locations of cross-sections.

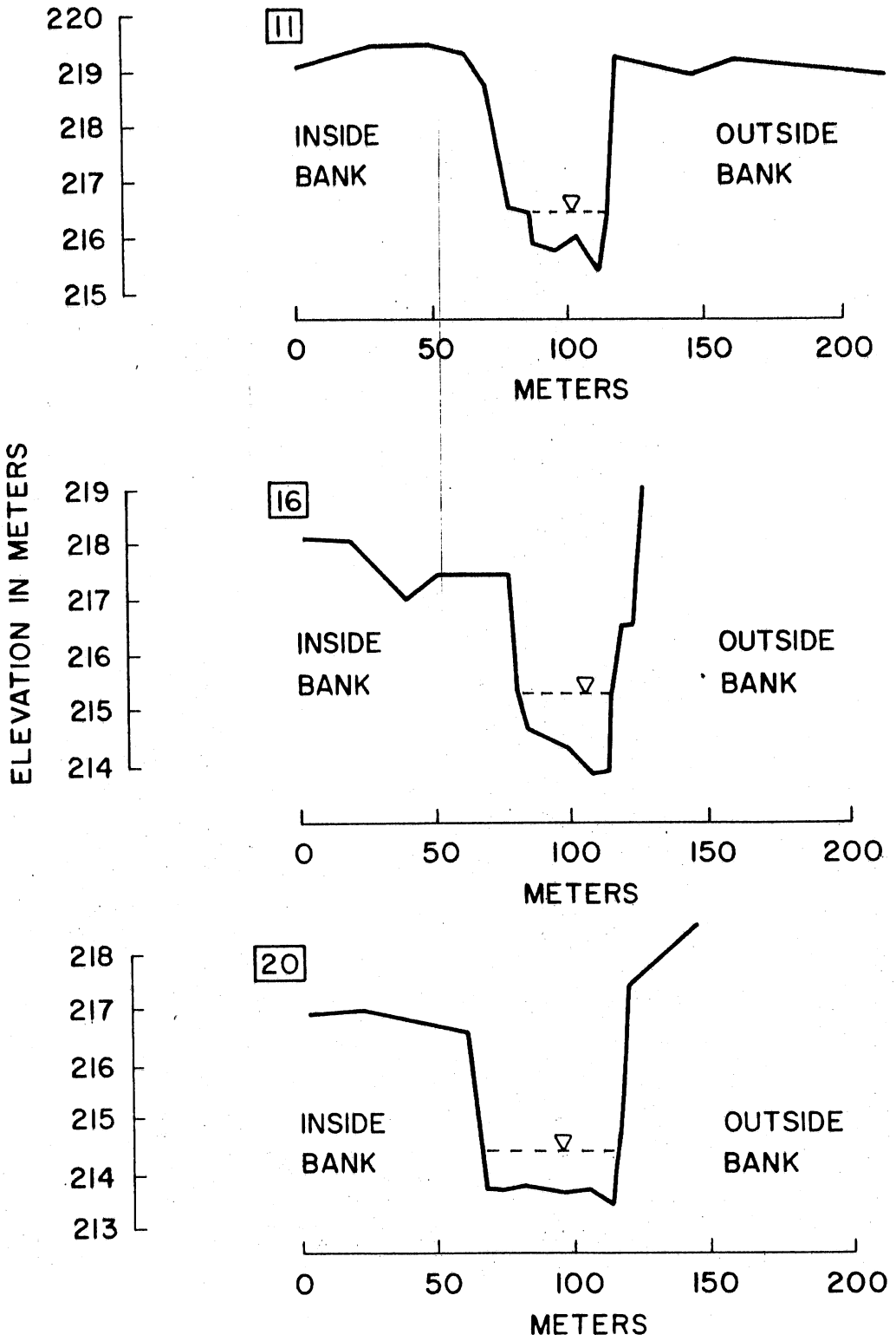

Fig. IV.6. Some typical cross-sections.

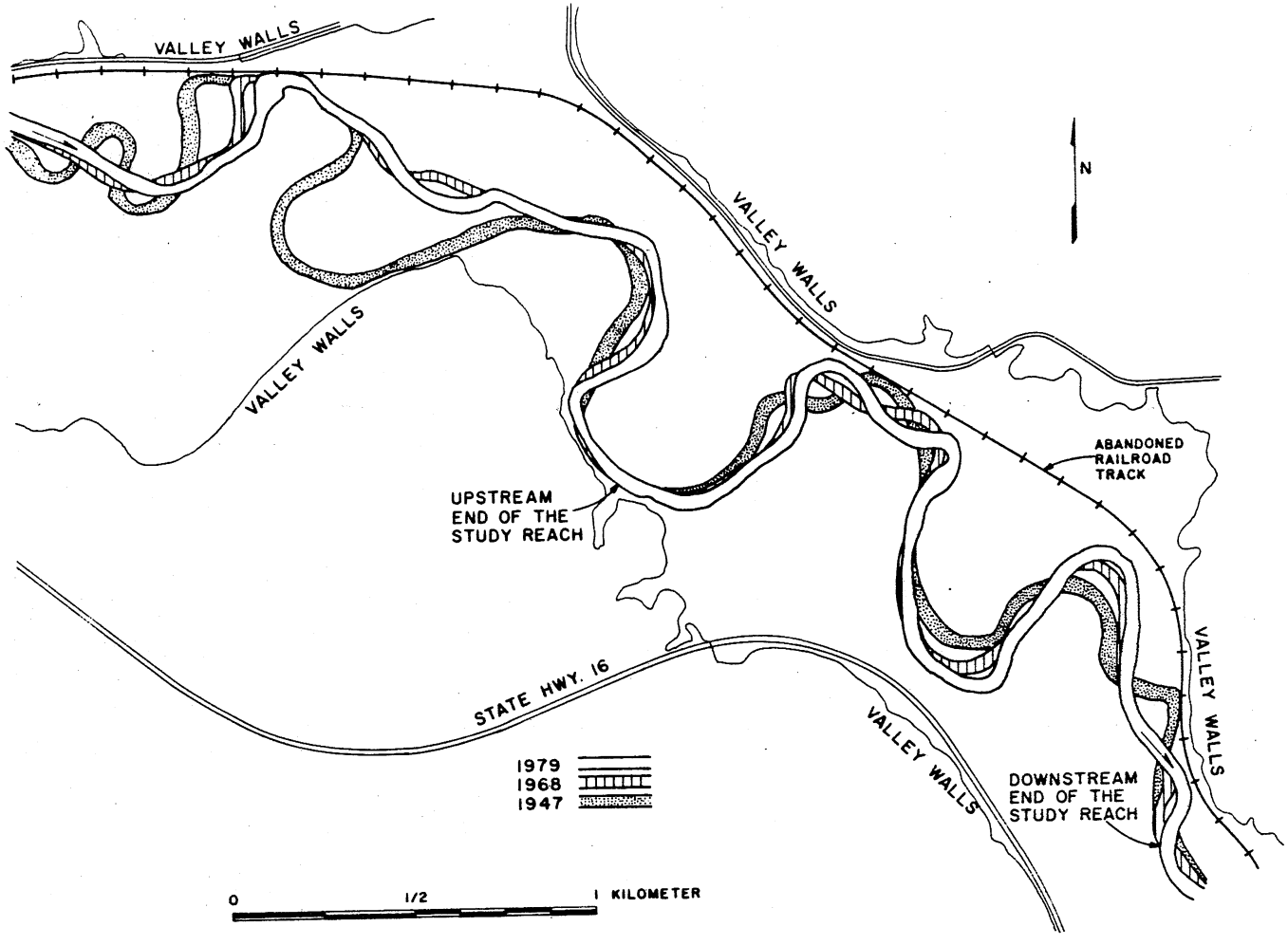

Fig. IV.7. The 1947, 1968, and 1979 channels of the Root River.

The results of this calibration are shown in Fig. IV.8. Forested and non-forested areas in that period are also indicated. The prediction of the model is seen to be satisfactory.

In order to check the calibration, the same set of values for E_o and C_f was used to calculate the movement of the river from 1947 to 1968. The results are shown in Fig. IV.9. The agreement between the calculated and the actual channel in 1968 is not as good as the agreement between the calculated and the actual channel in 1979. However, the model does give rather good results where the river shows the classical meandering pattern of bends that grow outward and shift downstream.

Finally, the model was used to predict the location of the channel in 2000. The same set of values for E_o and C_f was used. The results are shown in Fig. IV.10. The prediction suggests that the river will start to erode through the railroad track in two places within the next 10-20 years. The Minnesota Department of Natural Resources plans to develop a recreational path along the abandoned railroad track. The model can thus suggest where and when bank protection is needed.

C. Zumbro River Case Study

1. The Hydraulic and Geomorphic Setting

The Zumbro River, shown in Fig. IV.11, originates at Zumbro Lake, which is about 20 km north of Rochester. It flows in an easterly direction toward its confluence with the Mississippi River.

The reach chosen for the present computer analysis is located just west of Kellogg. It is approximately 7 km long.

The river valley. On the north side of the valley, the terrain rises to about 140 m above the valley bottom. On the south side of the valley there is a terrace, elevated about 30 m above the valley bottom. The valley has a bottom width of about 1.2 km and is filled with fine to medium sand.

Channel planform. For the period of record the sinuosity of the river, in the study area, has been fairly constant. It increased from 1.8 in 1938 to 1.9 in 1980. The river flows alternately through forested and non-forested areas. Throughout the period of record, the amount and location of non-forested areas along the river banks has changed. In 1938, non-forested areas were located along the river banks for about 19% of the length of the reach. In 1958 and 1980, the corresponding numbers were 9% and 5%.

Within the study area, the river is free to migrate except at the upstream and downstream ends where it impinges against the valley walls, as shown in Fig. IV.14.

Hydrology. The Zumbro River is not gaged within the length of the study reach. However, inferences as to hydrologic conditions could be made

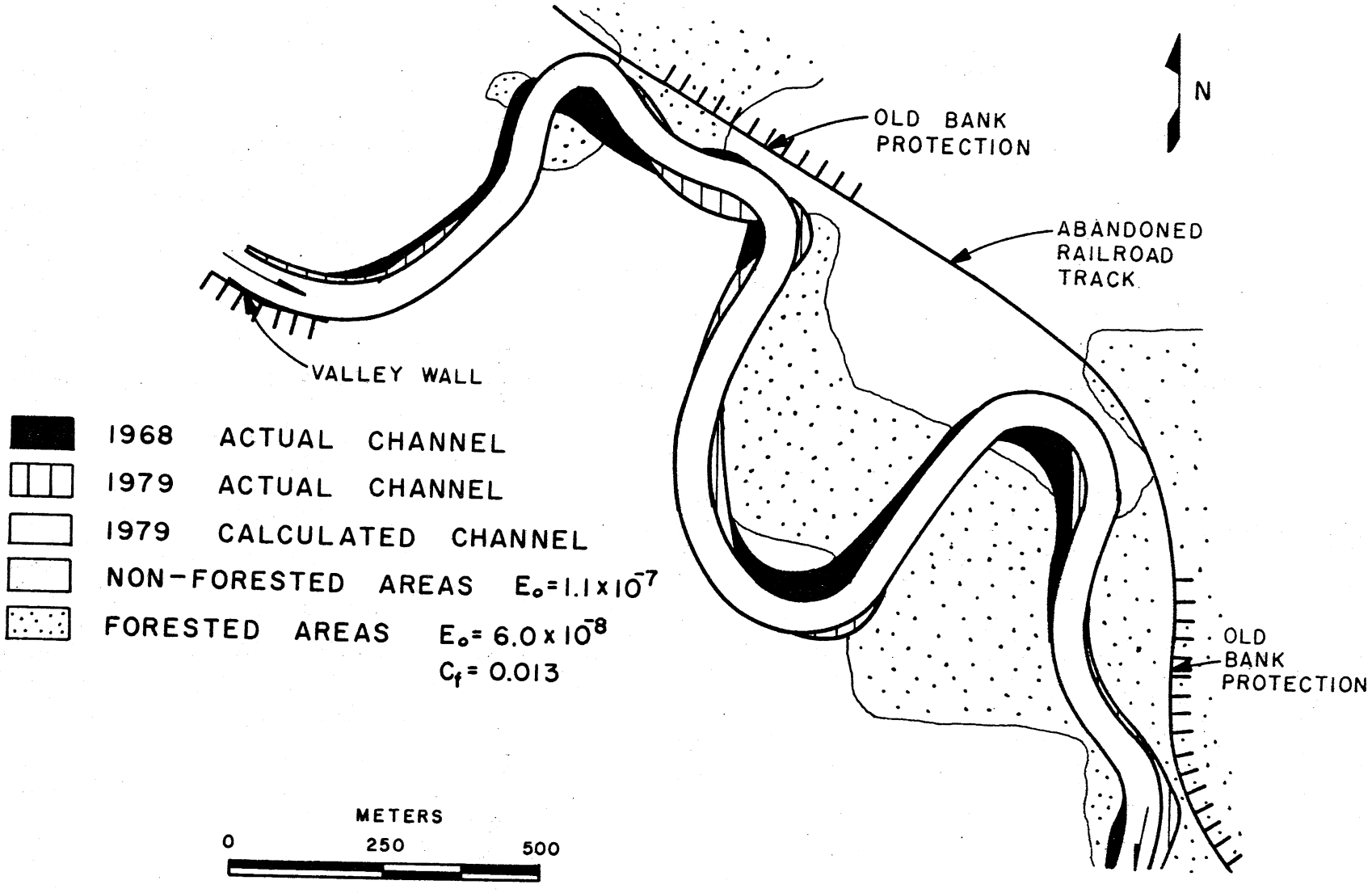

Fig. IV.8. Model calibration, using the period between 1968 - 1979.

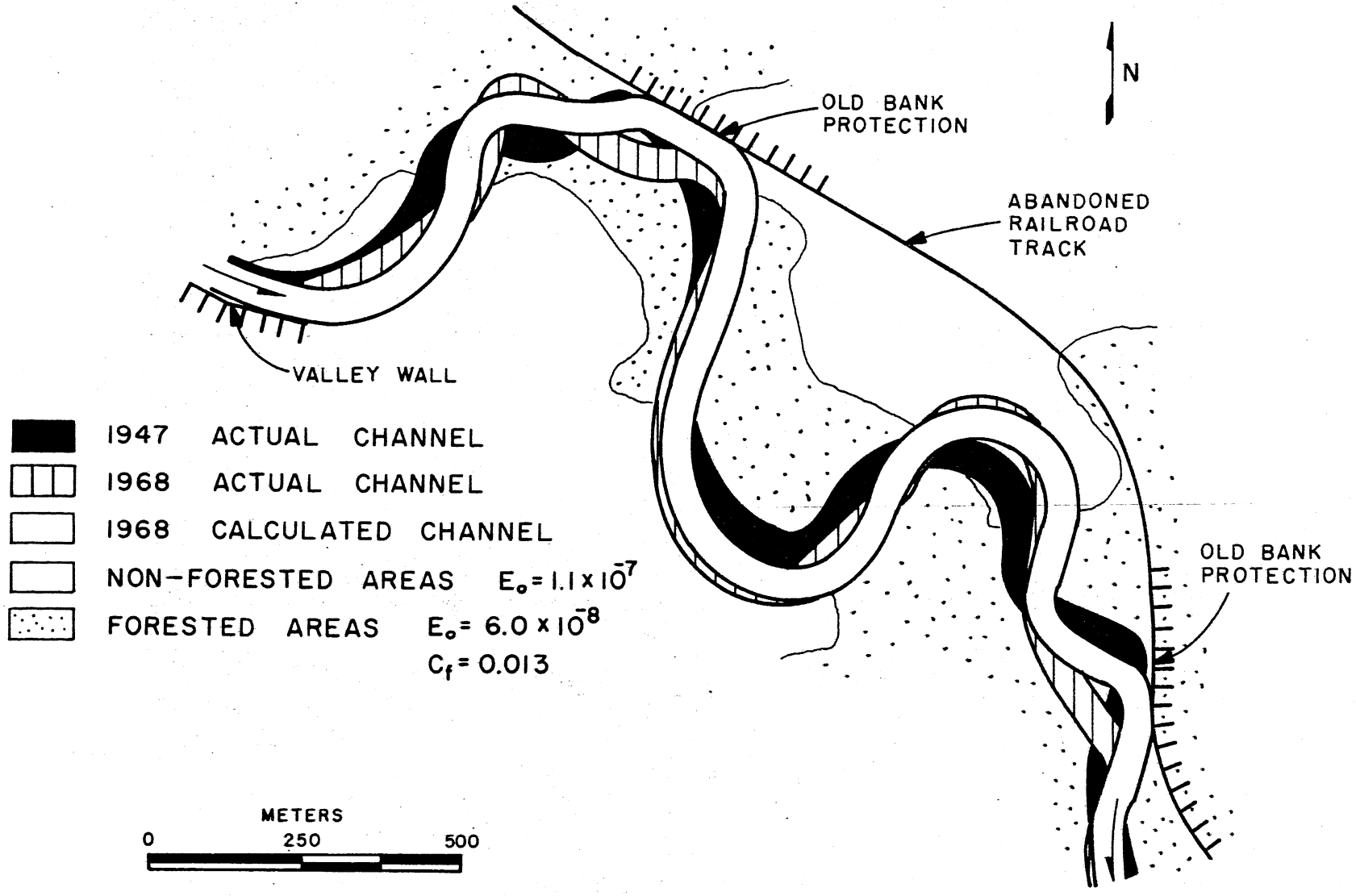

Fig. IV.9. Calibration verification, using the period between 1947 - 1968.

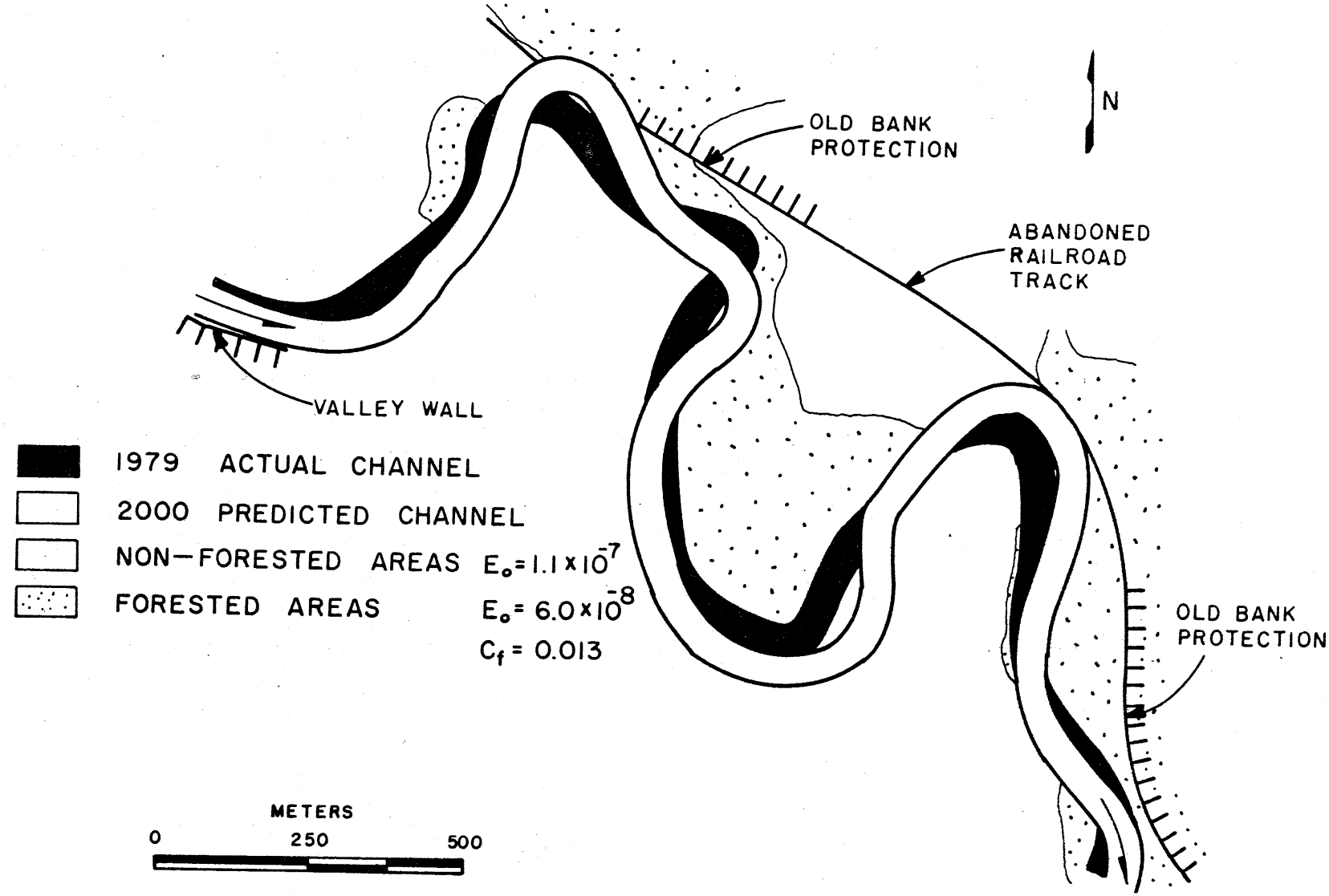

Fig. IV.10. Prediction from 1979 - 2000.

from the gaging stations at Zumbro Falls (operated from 1929 to 1980) and Kellogg (operated from 1975 to date), (Fig. IV.11). The difference in discharge between the study reach and Kellogg was assumed to be negligible due to the lack of substantial tributaries in between.

Since the gaging station at Kellogg has only been in operation for 10 years, data for various flood flows at Zumbro Falls was used to estimate flood flows at Kellogg. The following relation from Guetzkow [1977], which is applicable to most areas in Minnesota, was used.

$$Q_u = Q_g(A_u/A_g)^{0.6} \tag{37}$$

Where: Q_u = Flow rate at the ungaged site.

Q_g = Flow rate at the gaged site.

A_u = Drainage area for the ungaged site = 3630 km^2 for Kellogg.

A_g = Drainage area for the gaged site = 2930 km^2 for Zumbro Falls.

Data for various flood flows are listed in Table 5. The information for Zumbro Falls was compiled by the U.S. Geological Survey.

A rating curve was obtained for the gage site at Kellogg. This, together with cross-section data obtained upstream of the gaging station (Fig. IV.12), allowed for an estimate of bankfull flow in the study reach.

Channel geometry. Several cross-sections just downstream of the study reach were surveyed in 1960 by the St. Paul District of the U.S. Army Corps of Engineers. Locations of these cross-sections are shown in Fig. VI.12. Some typical cross-sections are shown in Fig. IV.13, and cross-section characteristics are listed in Table 6. These measurements, together with a topographical map, allowed for estimation of average bankfull geometry and flow parameters for the river reach between cross-sections No. 28 and 41, as shown in Table 7. This reach had a sinuosity equal to 1.44 in 1960. Bankfull geometry and flow parameters that would result if the river were straight, $S_i = 1$, were computed for the reach between cross-sections No. 28 and 41. They are assumed to be the same for the study reach. These parameters were used as input data in the program, and are listed in Table 7.

2. History of Channel Planform

Aerial photographs of the channel for the years 1938, 1951, 1958, 1964, 1971, 1980, and a topographical map based on aerial photographs from 1973 and 1974 were obtained. The topographical map and the aerial photographs from 1938, 1958, and 1980 were enlarged to a common scale. In Fig. IV.14, the 1938, 1958, and 1980 channels are shown. The river showed a typical meandering behavior throughout the period of record.

It can be seen from Fig. IV.14 that the river generally migrated more between 1938 to 1958 than between 1958 to 1980, although the latter period is slightly longer. This will be discussed further in connection with the computer analysis.

TABLE 5. VARIOUS FLOOD FLOWS FOR THE ZUMBRO RIVER

Flow	Discharge at Zumbro Falls (m^3/s)	Discharge at Kellogg (m^3/s)
bankfull		450
2-year	290	330
5-year	490	560
10-year	640	720
25-year	830	950
50-year	980	1120
100-year	1140	1290
largest on record	1020	1160

TABLE 6. CROSS-SECTION CHARACTERISTICS

Cross-section Number	Top Width (m)	Mean Depth (m)
28	67	3.5
29	98	2.9
30	96	2.8
31	--	--- (Not typical)
32	--	--- (Not typical)
33	49	3.5
34	57	3.0
35	64	3.3
36	72	3.1
37	--	--- (Not typical)
38	53	3.7
39	52	3.3
40	69	3.0
41	38	3.3

TABLE 7. AVERAGE PARAMETERS AT BANKFULL FLOW

	River Channel	Straight Channel
Water surface slope	$I = 6.20 \cdot 10^{-4}$	$I_o = 8.93 \cdot 10^{-4}$
Channel width	$B = 65.0$ m	$B_o = 65.0$ m
Mean depth	$H = 3.22$ m	$H_o = 2.85$ m
Discharge	$Q = 450$ m^3/s	$Q_o = 450$ m^3/s
Mean flow velocity	$U = 2.15$ m/s	$U_o = 2.43$ m/s
Froude number	$F = 0.38$	$F_o = 0.46$

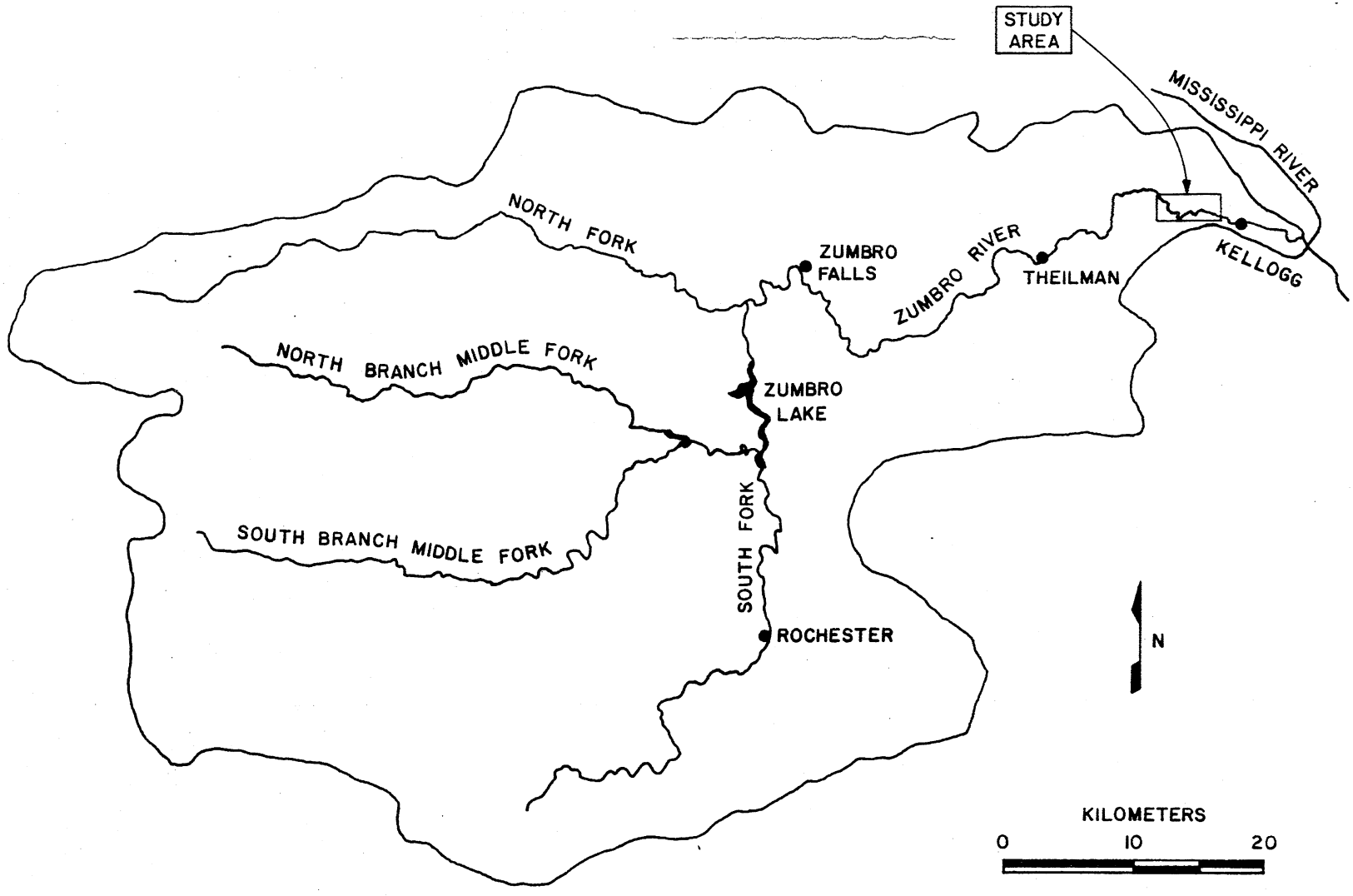

Fig.IV.11. The Zumbro River watershed.

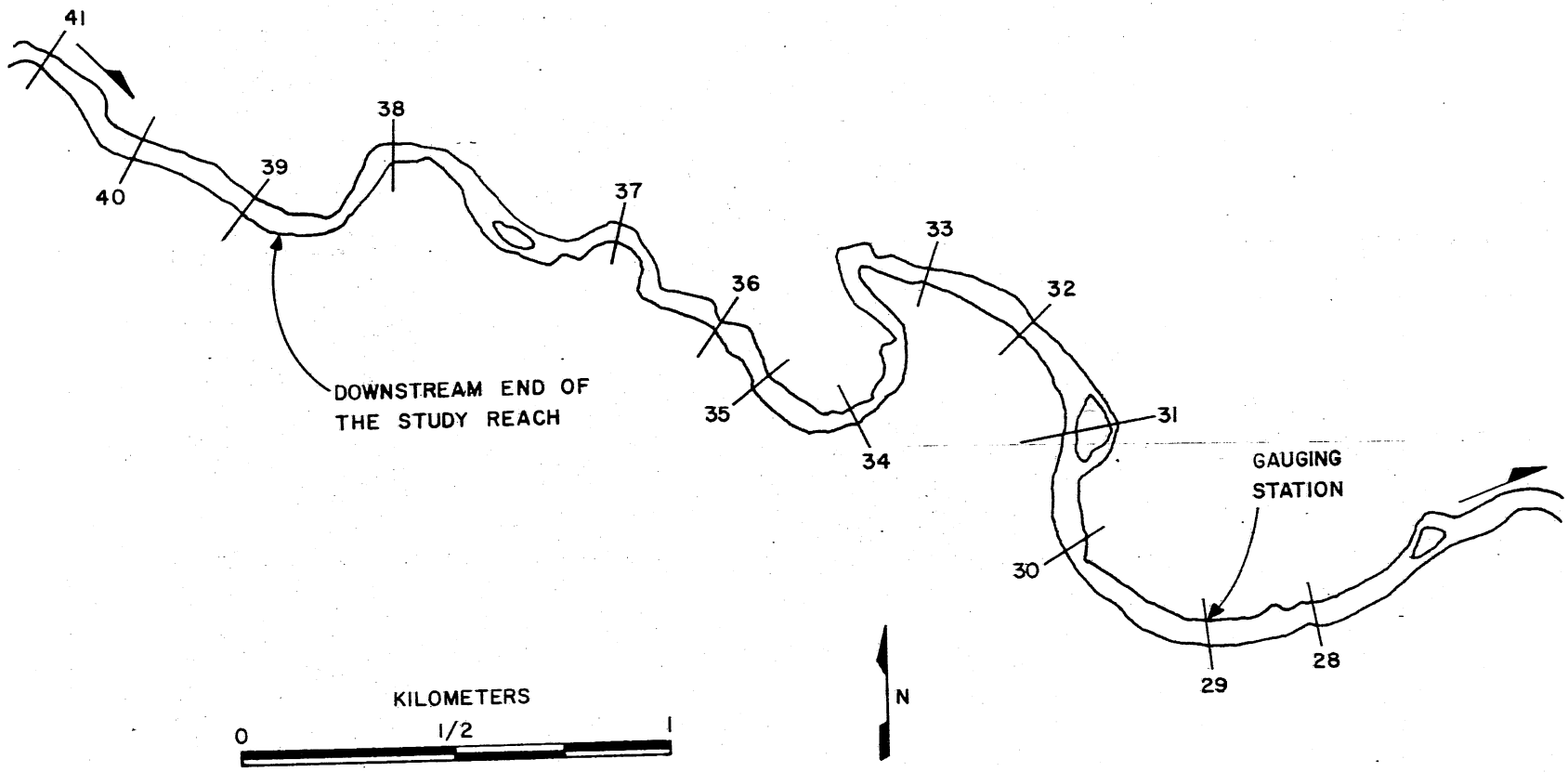

Fig. IV.12. Locations of cross-sections.

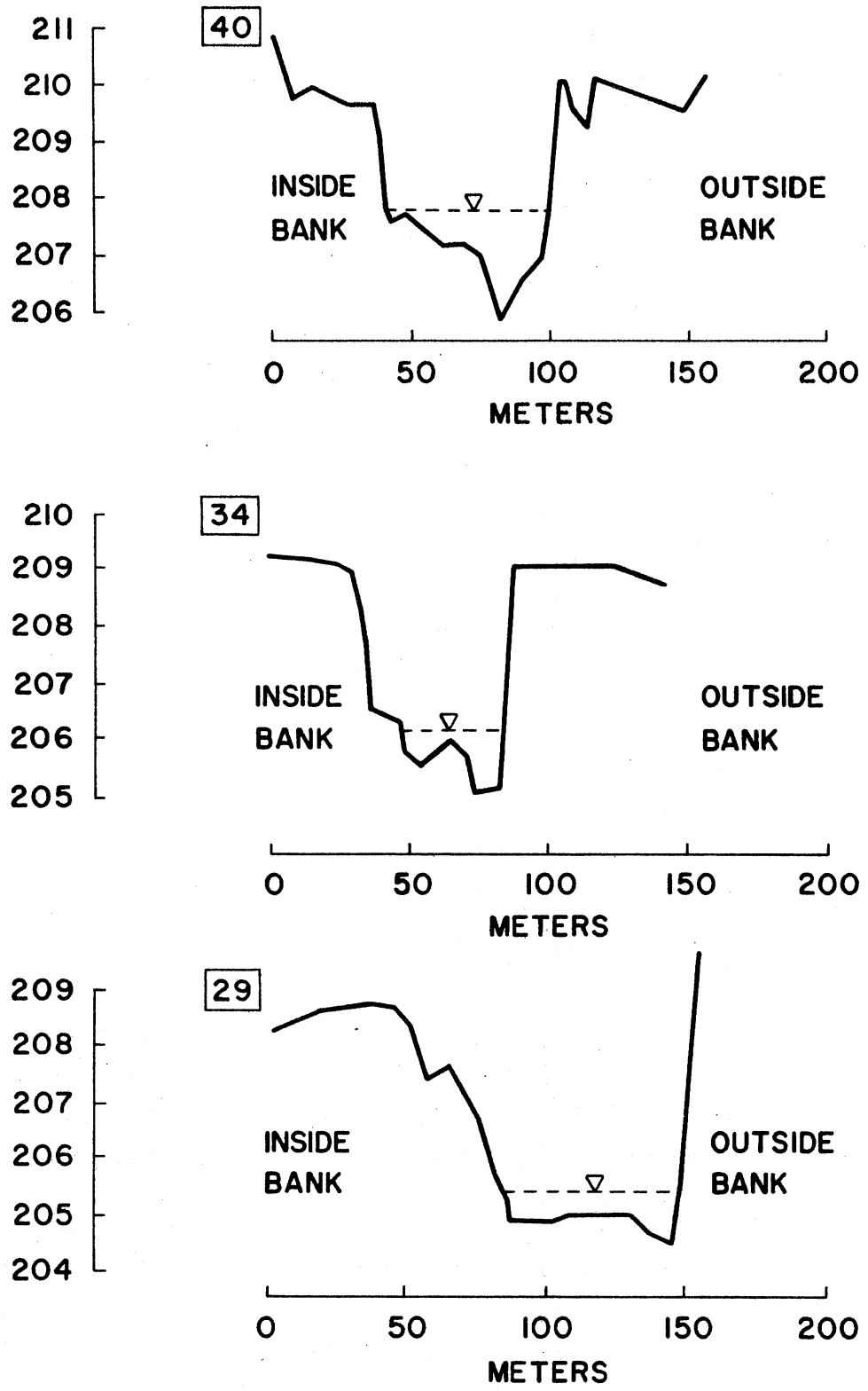

Fig.IV.13. Some typical cross-sections.

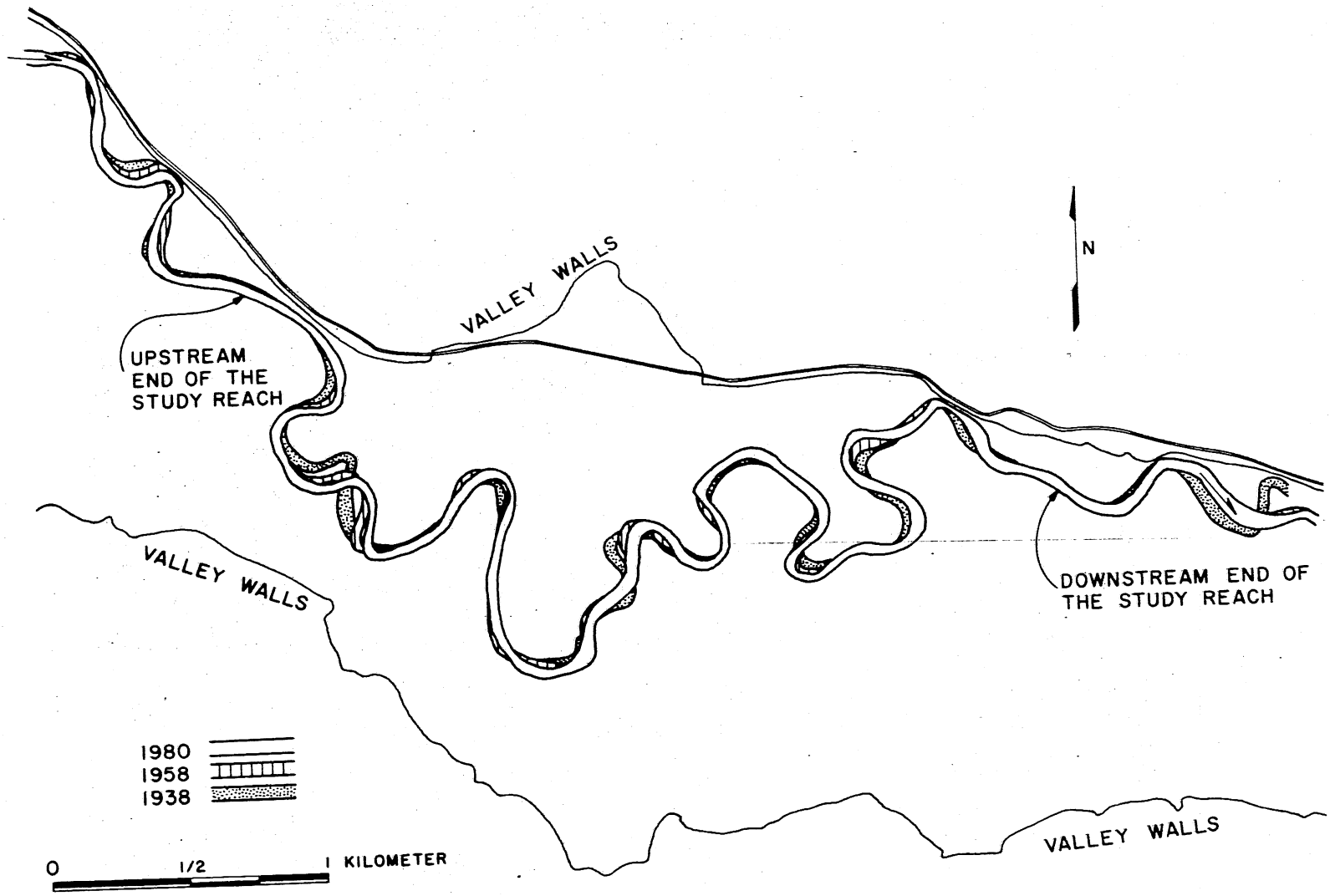

Fig. IV.14. The 1938, 1958, and 1980 channels of the Zumbro River.

3. Computer Analysis

The model was calibrated by optimizing the erosion coefficient, E_o, and the dimensionless friction factor, C_f. The period between 1938 and 1958 was used for the calibration and following values were obtained:

Non-forested areas $E_o = 7.0 \cdot 10^{-8}$

Forested areas $E_o = 2.5 \cdot 10^{-8}$

$C_f = 0.020$

The results of this calibration are shown in Fig. IV.15. Forested and non-forested areas in that period are also indicated. The prediction of the model is seen to be reasonable.

As expected, the model overestimates migration for the period between 1958 and 1980 if the same set of constants is used. The results of using the same value for C_f, but reducing the values of the erosion coefficient by 30%, are shown in Fig. IV.16.

Non-forested areas $E_o = 4.9 \cdot 10^{-8}$

Forested areas $E_o = 1.8 \cdot 10^{-8}$

The prediction of the model is seen to be satisfactory. One possible reason was found that might explain these reduced erosion values: By comparing aerial photographs for these two periods, it was observed that the forest was much denser in the latter period. This may account for lower erosion values for that period, at least for the forested areas.

Finally, the model was used to predict the location of the channel in 2000. The same set of values for C_f and E_o was used as for the period between 1958 and 1980. The results are shown in Fig. IV.17.

D. Minnesota River Case Study

1. The Hydraulic and Geomorphic Setting

The Minnesota River, shown in Fig. IV.18, originates at Big Stone Lake near the border of Minnesota and South Dakota. From its source to Mankato, it flows in a southeasterly direction. At Mankato, it abruptly changes direction and flows northeasterly toward its confluence with the Mississippi River.

The reach chosen for the present computer analysis is located just north of Mankato. It is approximately 3.9 km long.

The river valley. Along the study reach, the Minnesota River has roughly straight, parallel walls (Fig. IV.21). The valley has a bottom width of about 1.4 km. The west wall is elevated approximately 50 m, and the east wall about 30 m, above the valley bottom.

Borehole logs obtained from the Minnesota Geological Survey suggest that the valley around Mankato has a 3 m thick topsoil of clayey silt.

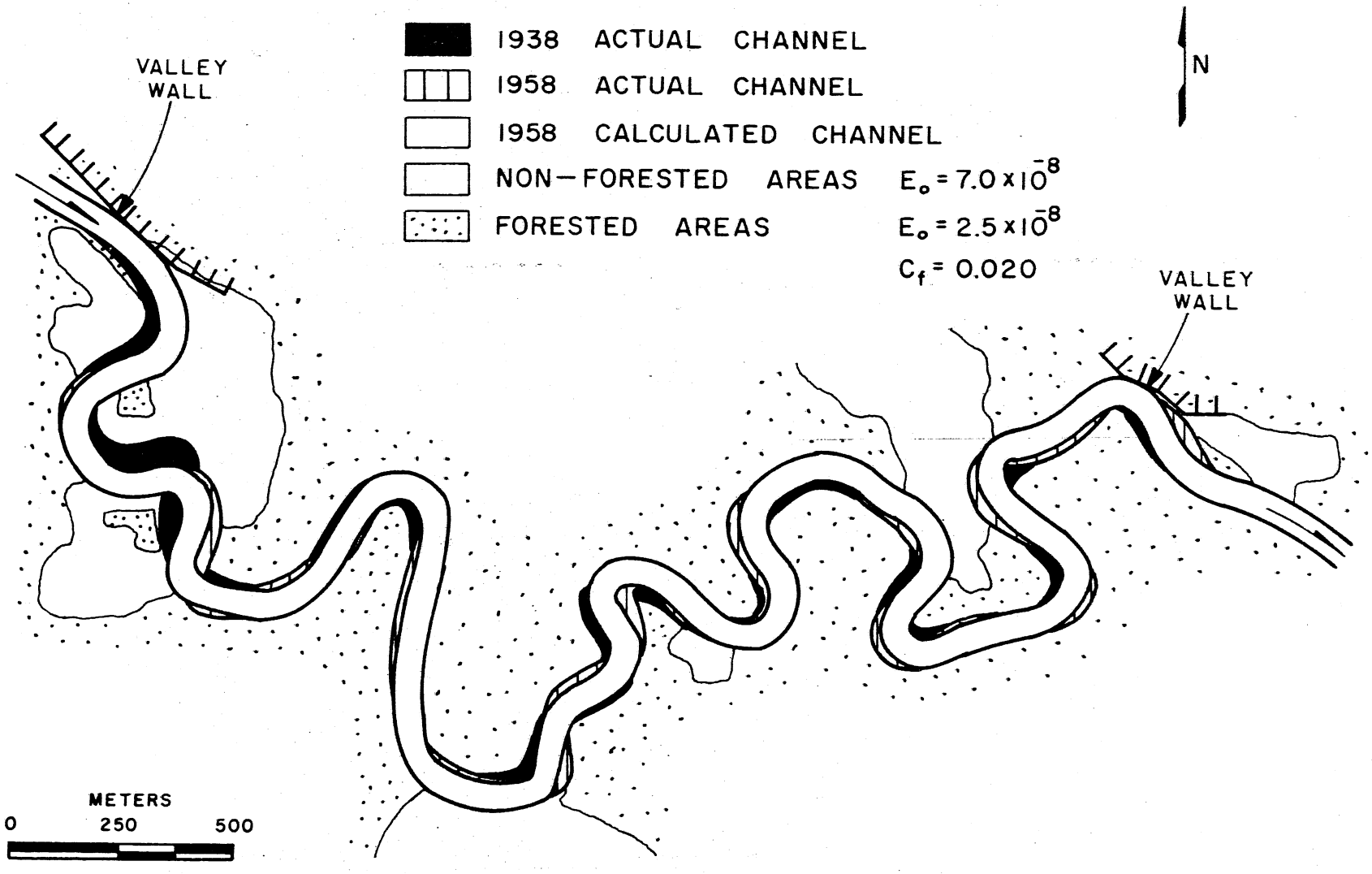

Fig. IV.15. Model calibration, using the period between 1938 - 1958.

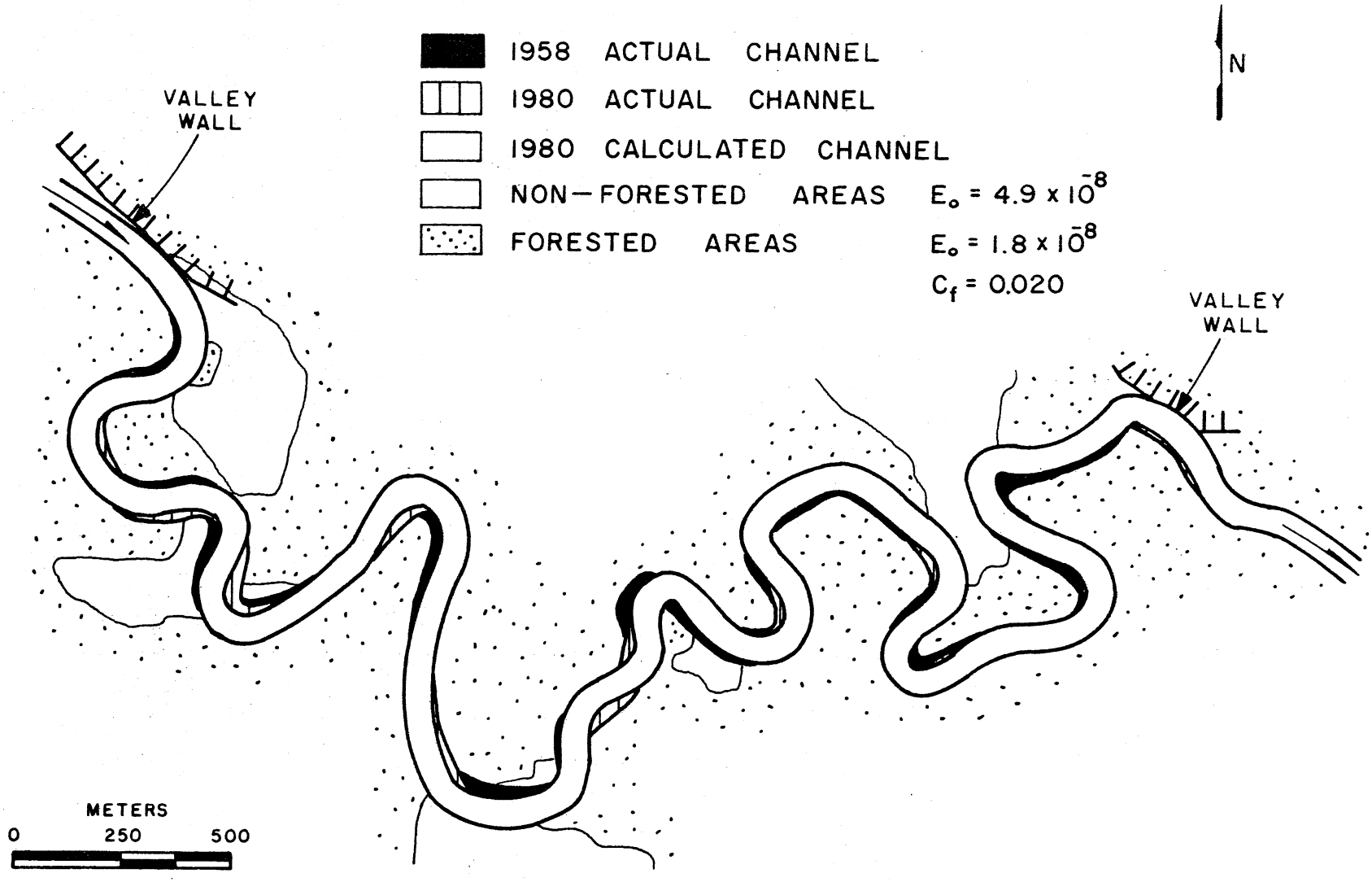

Fig. IV.16. Calibration verification, using the period between 1958 - 1980.

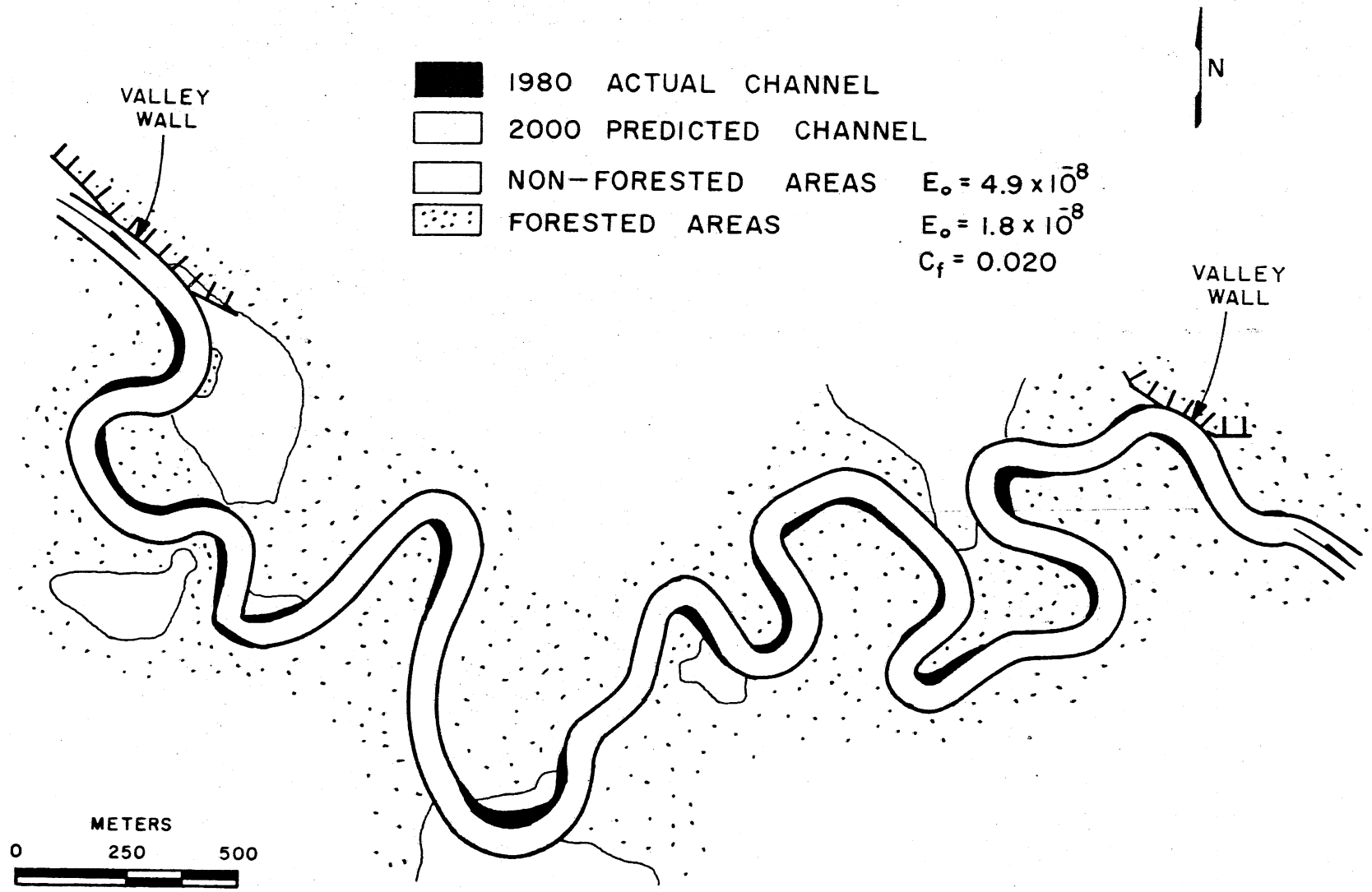

Fig. IV.17. Prediction from 1980 - 2000.

Below the topsoil there are 6 m of medium sand and then 8 m of medium to coarse sand.

Channel planform. From 1938 to 1980 the sinuosity of the river increased, from 1.5 to 1.9, in the study area. The river flows alternately through forested and non-forested areas. Throughout the period of record, the amount and location of non-forested areas along the river banks has changed. In 1938, non-forested areas were located along the river banks for about 43% of the length of the reach. In 1961 and 1980, the corresponding values were 44% and 50%.

Within the study area the river is free to migrate, except at one location where it impinges against the east valley wall (Fig. IV.21).

Hydrology. The Minnesota River is not gaged within the length of the study reach. However, inferences as to hydrologic conditions could be made from the gaging station at Mankato (Fig. IV.18). This gaging station has been in operation since 1903. The difference in discharge between the study reach and Mankato was assumed to be negligible due to the lack of substantial tributaries in between. Data for various flood flows are listed in Table 8; the information was compiled by the U.S. Geological Survey.

A rating curve was obtained for the gage site at Mankato. This, together with cross-section data obtained downstream of the gaging station (Fig. IV.19), allowed for an estimate of bankfull flow in the study reach.

Channel geometry. Several cross-sections within and close to the study reach were surveyed between 1966 and 1984 by the St. Paul District of the U.S. Army Corps of Engineers. Locations of these cross-sections are shown in Fig. IV.19. Some typical cross-sections are shown in Fig. IV.20, and cross-section characteristics are listed in Table 9. These measurements, together with a topographical map, allowed for estimation of average bankfull geometry and flow parameters for the river reach between cross-sections No. 74 and 17200, as shown in Table 10. This reach had a sinuosity approximately equal to 1.67. Bankfull geometry and flow parameters that would result if the river were straight, $S_i = 1$, were computed for the reach between cross-sections No. 74 and 17200. They were assumed to be the same for the study reach. These parameters were used as input data in the program, and are listed in Table 10.

2. History of Channel Planform

Aerial photogaphs of the channel for the years 1938, 1950, 1958, 1961, 1964, 1968, 1980, and a topographical map based on aerial photographs from 1963, 1973 and 1977 were obtained. The topographical map and the aerial photographs from 1938, 1961, and 1980 were enlarged to a common scale. In Fig. IV.21, the 1938, 1961, and 1980 channels are shown.

Within the study reach, the river showed a typical meandering behavior and migrated very actively throughout the period of record. Downstream of the study reach there are two straight reaches that showed very little movement between 1938 and 1980. No obvious reason was found that accounted for this stability. Between these two straight reaches mentioned above,

TABLE 8. VARIOUS FLOOD FLOWS FOR THE MINNESOTA RIVER

Flow	Discharge at Mankato (m^3/s)
bankfull	560
2-year	410
5-year	800
10-year	1100
25-year	1510
50-year	1830
100-year	2160
largest on record	2660

TABLE 9. CROSS-SECTION CHARACTERISTICS

Cross-section Number	Top Width (m)	Mean Depth (m)
74	94	5.3
75	114	4.6
76	109	4.2
77	79	4.5
78	103	5.0
80	---	--- (Not typical)
81	118	4.2
85	104	3.3
87	104	3.3
700	---	--- (Not typical)
4130	---	--- (Not typical)
9050	104	4.7
11650	84	5.2
14200	140	4.9
15870	105	4.4
17200	---	--- (Not typical)

TABLE 10. AVERAGE PARAMETERS AT BANKFULL FLOW

	River Channel	Straight Channel
Water surface slope	$I = 1.86 \cdot 10^{-4}$	$I_o = 3.10 \cdot 10^{-4}$
Channel width	$B = 104.8$ m	$B_o = 104.8$ m
Mean depth	$H = 4.47$ m	$H_o = 3.77$ m
Discharge	$Q = 560$ m^3/s	$Q_o = 560$ m^3/s
Mean flow velocity	$U = 1.20$ m/s	$U_o = 1.43$ m/s
Froude number	$F = 0.18$	$F_o = 0.24$

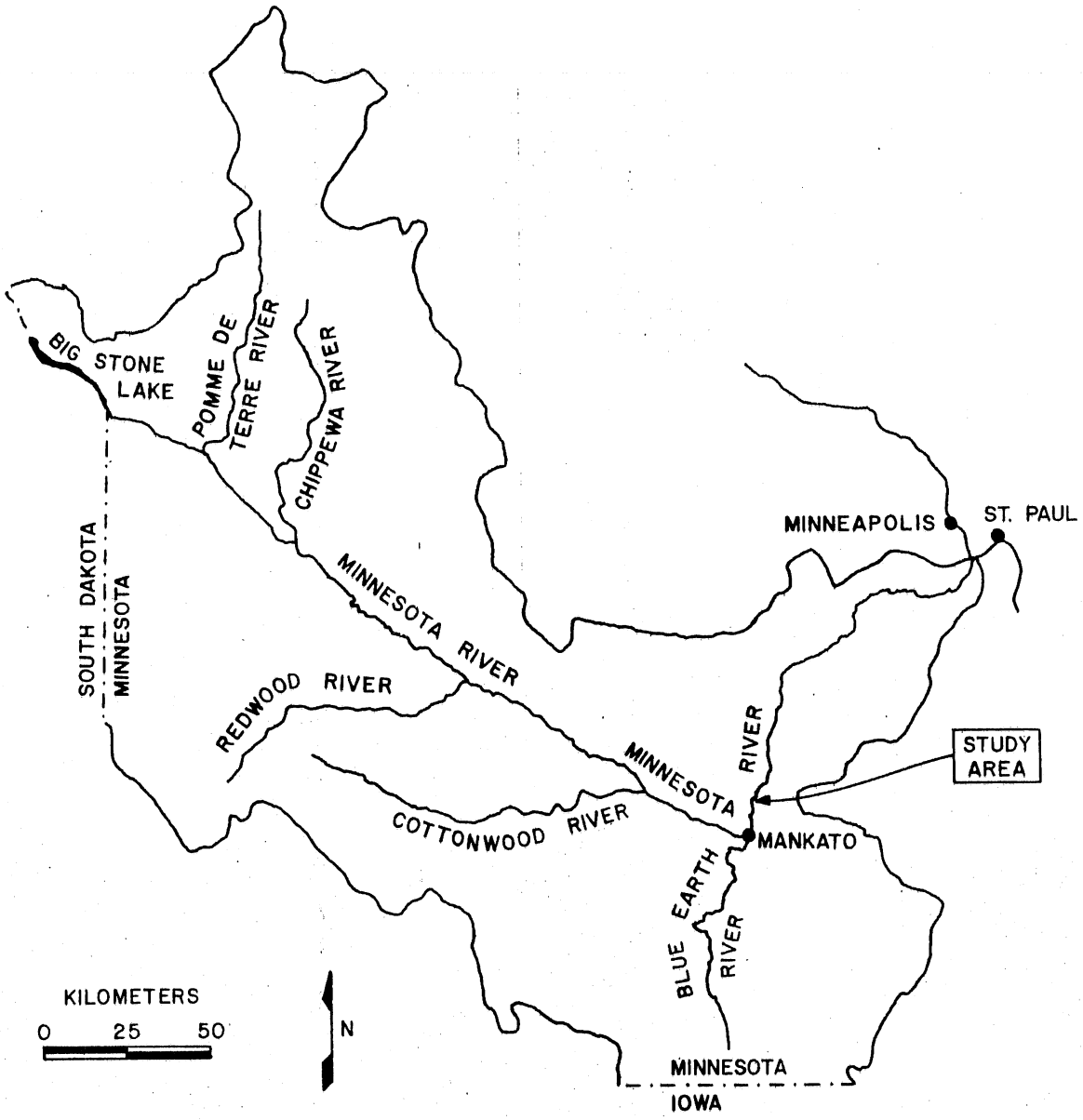

Fig. IV.18. The Minnesota River Watershed.

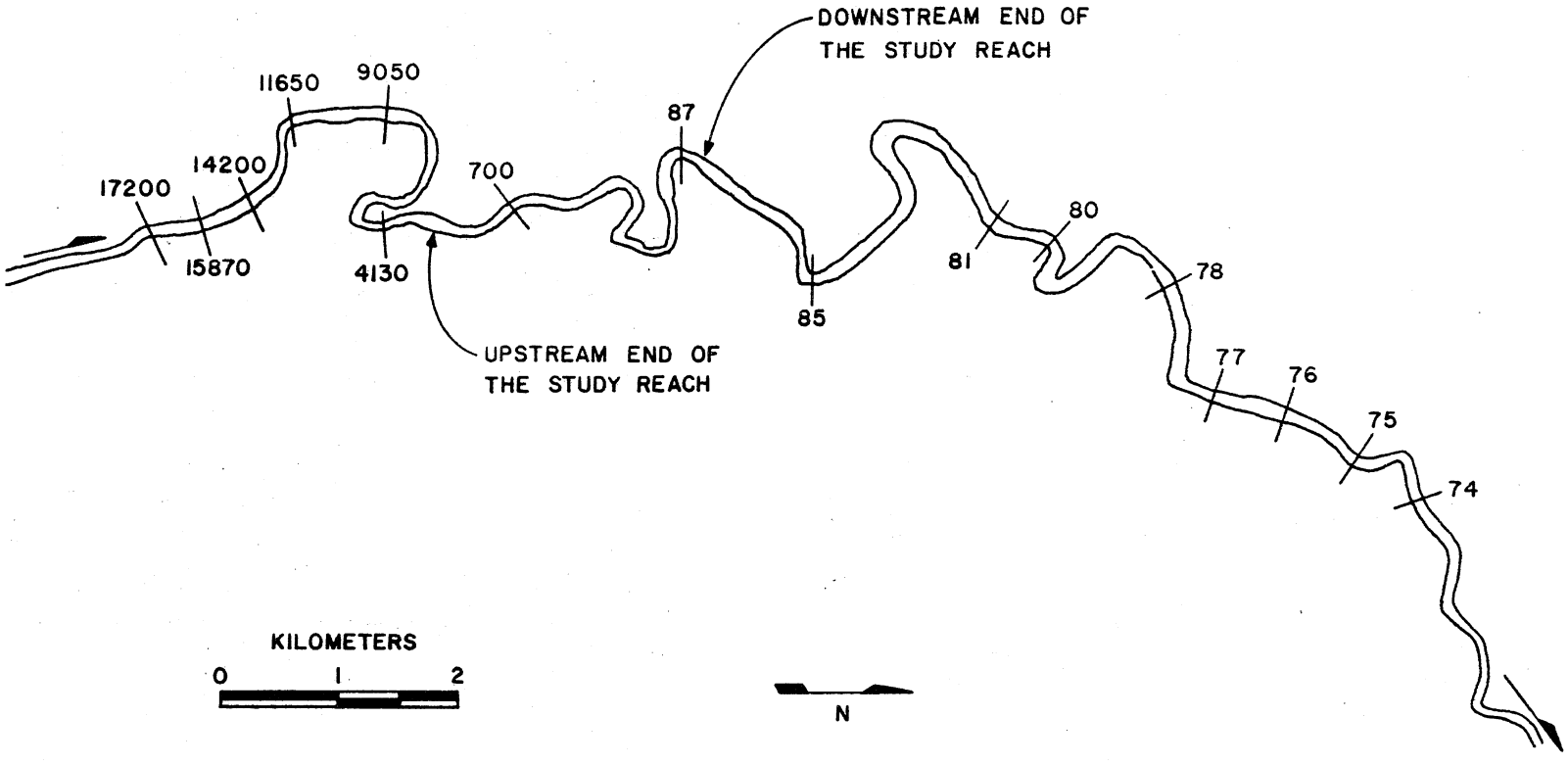

Fig. IV.19. Locations of cross-sections.

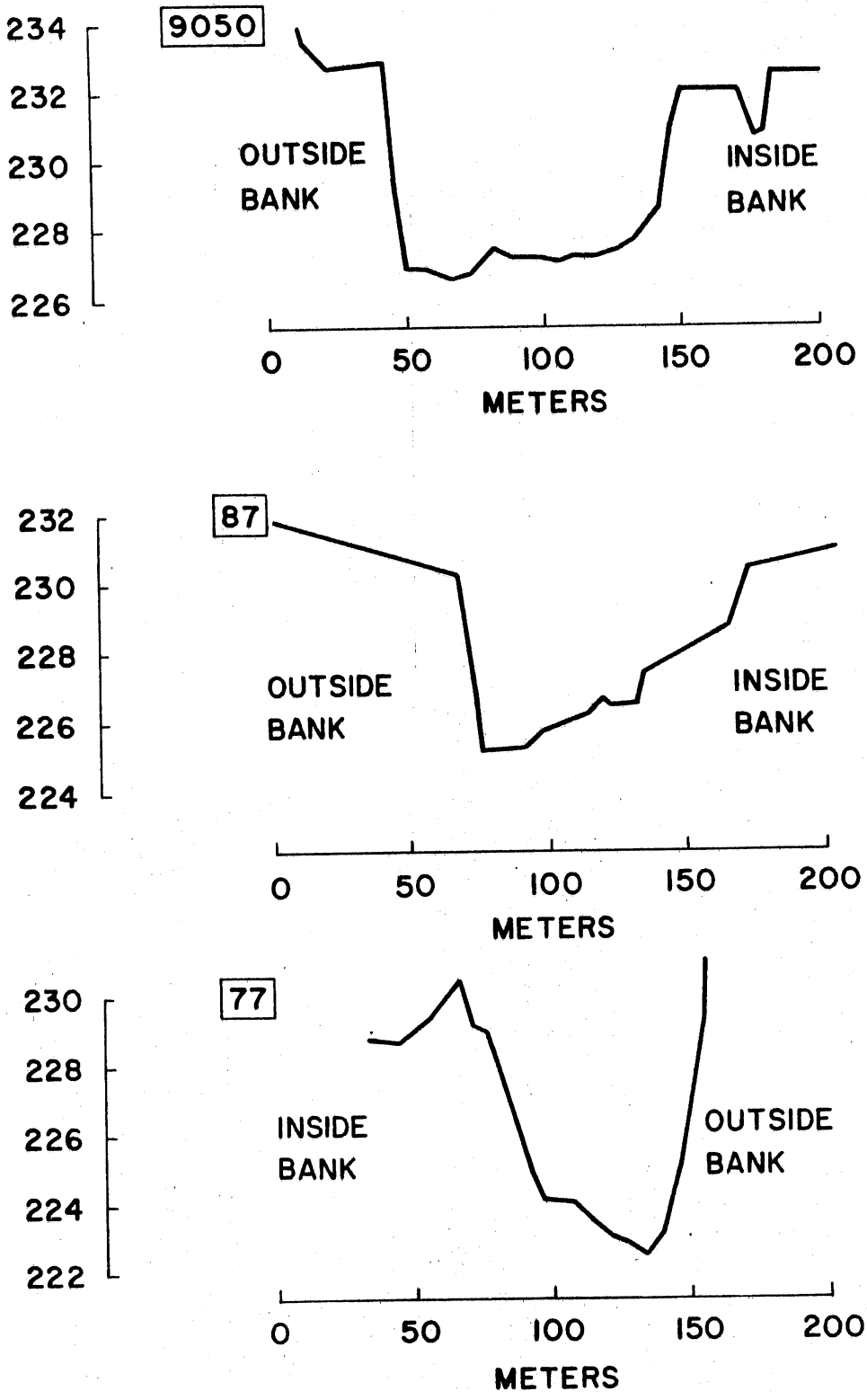

Fig. IV.20. Some typical cross-sections.

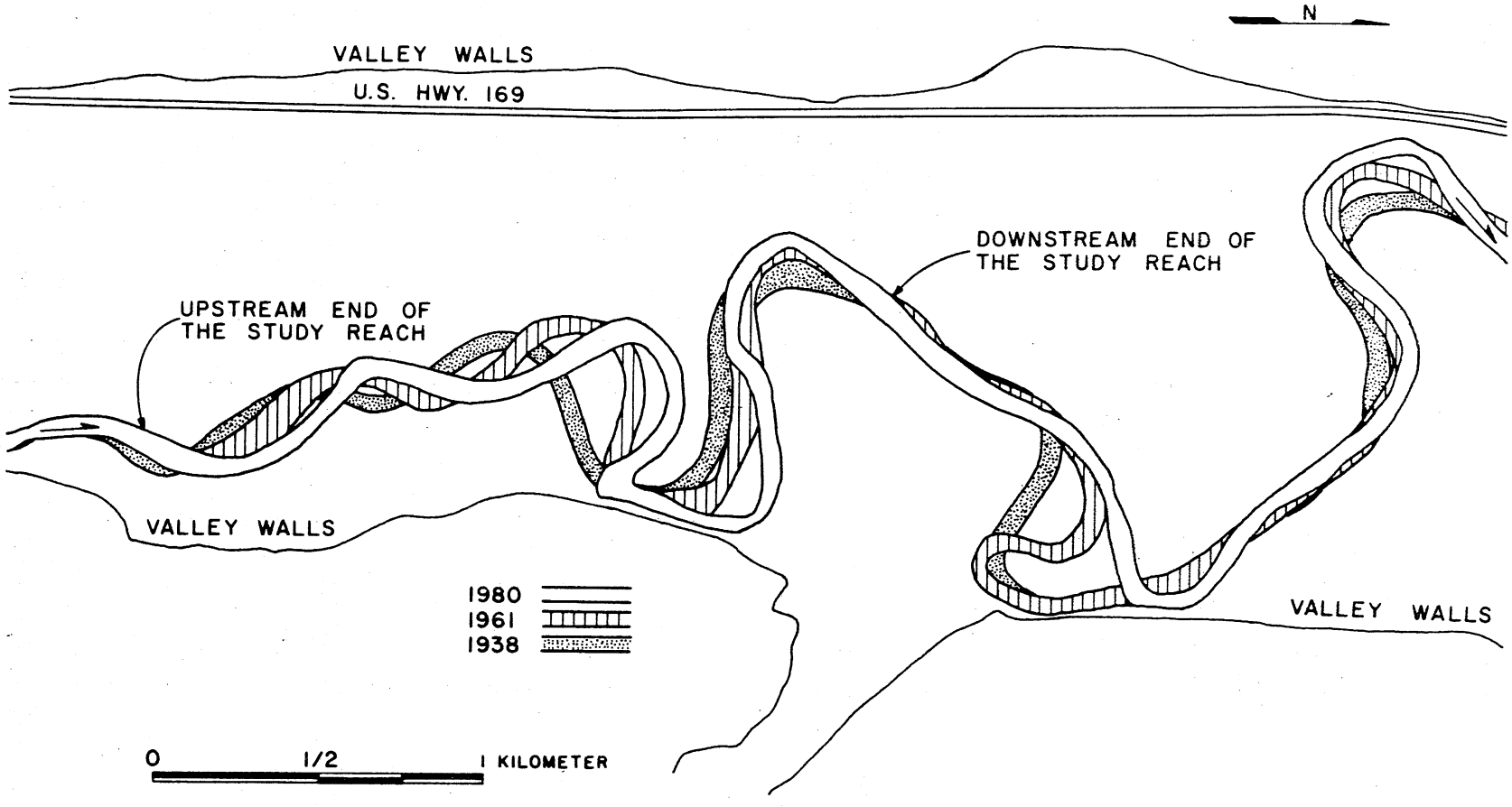

Fig. IV.21. The 1938, 1961, and 1980 channels of the Minnesota River.

there is a very active bend. This bend cut itself off sometime between 1961 and 1964.

3. Computer Analysis

The model was calibrated by optimizing the erosion coefficient, E_o, and the dimensionless friction factor, C_f. The period between 1938 and 1961 was used for the calculation and following values were obtained:

Non-forested areas $E_o = 2.5 \cdot 10^{-7}$

Forested areas $E_o = 2.5 \cdot 10^{-7}$

$C_f = 0.012$

Since the upstream end was curved in 1938, as shown in Fig. IV.21, a non-uniform velocity distribution at the upstream end was assumed. A value of $u'_b(0) = 0.3U_o$ was found to give good results. $u'_b(0)$ is the difference between the velocity at the left bank and the mean velocity. The influence of this assumption decays with increasing distance from the upstream end and vanishes by about 0.6 km from the upstream end. The results of this calibration are shown in Fig. IV.22. Forested and non-forested areas in that period are also indicated. The prediction of the model is not good. The model is able to predict the correct direction of the migration everywhere, but it is not able to simulate the correct magnitude of movement for each bend.

In order to check the calibration, the same set of values for E_o and C_f was used to calculate the movement of the river from 1961 to 1980. A uniform velocity distribution was assumed at the upstream end since that end was almost straight in 1961. The results of this calculation are shown in Fig. IV.23. The agreement between the calculated and the actual channel in 1980 is rather good. The model gives much better results than it gave for the earlier period.

Finally, the model was used to predict the location of the channel in 2000. The same set of values for E_o and C_f was used. Again, a uniform velocity distribution was assumed at the upstream end. The results are shown in Fig. IV.24. It can be seen that the model indicates a cutoff sometime around 2000.

E. Red Lake River Case Study

1. The Hydraulic and Geomorphic Setting

The Red Lake River, shown in Fig. IV.25, originates at Lower Red Lake, which is about 100 km east of Crookston. It meanders south and west, and empties into the Red River at East Grand Forks.

The reach chosen for the present computer analysis is located just east of Crookston. It is approximately 4.2 km long.

The river valley. Along the study reach, the river valley is very irregular. It has a shape imposed by the current and previous meandering

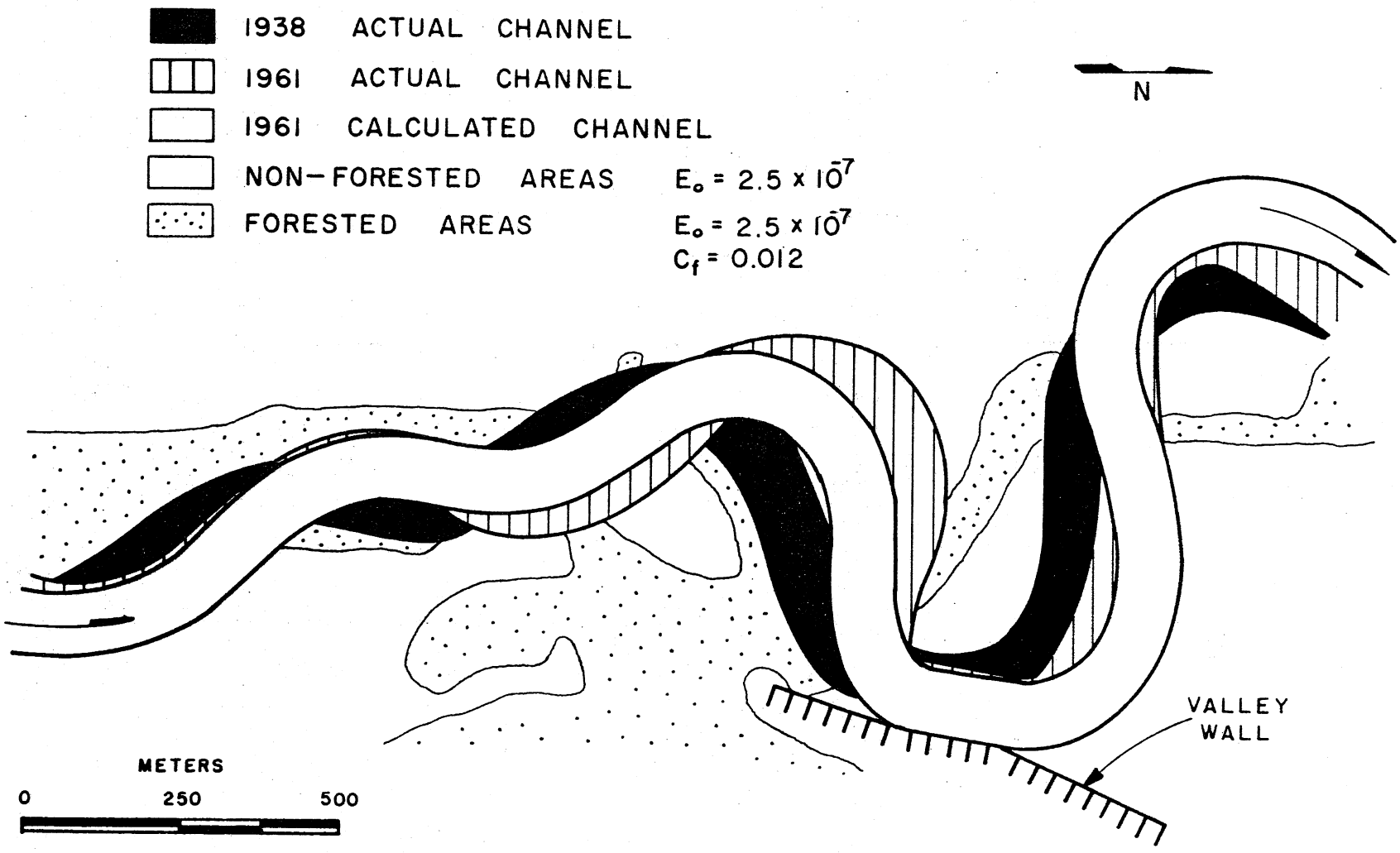

Fig. IV.22. Model calibration, using the period between 1938 - 1961.

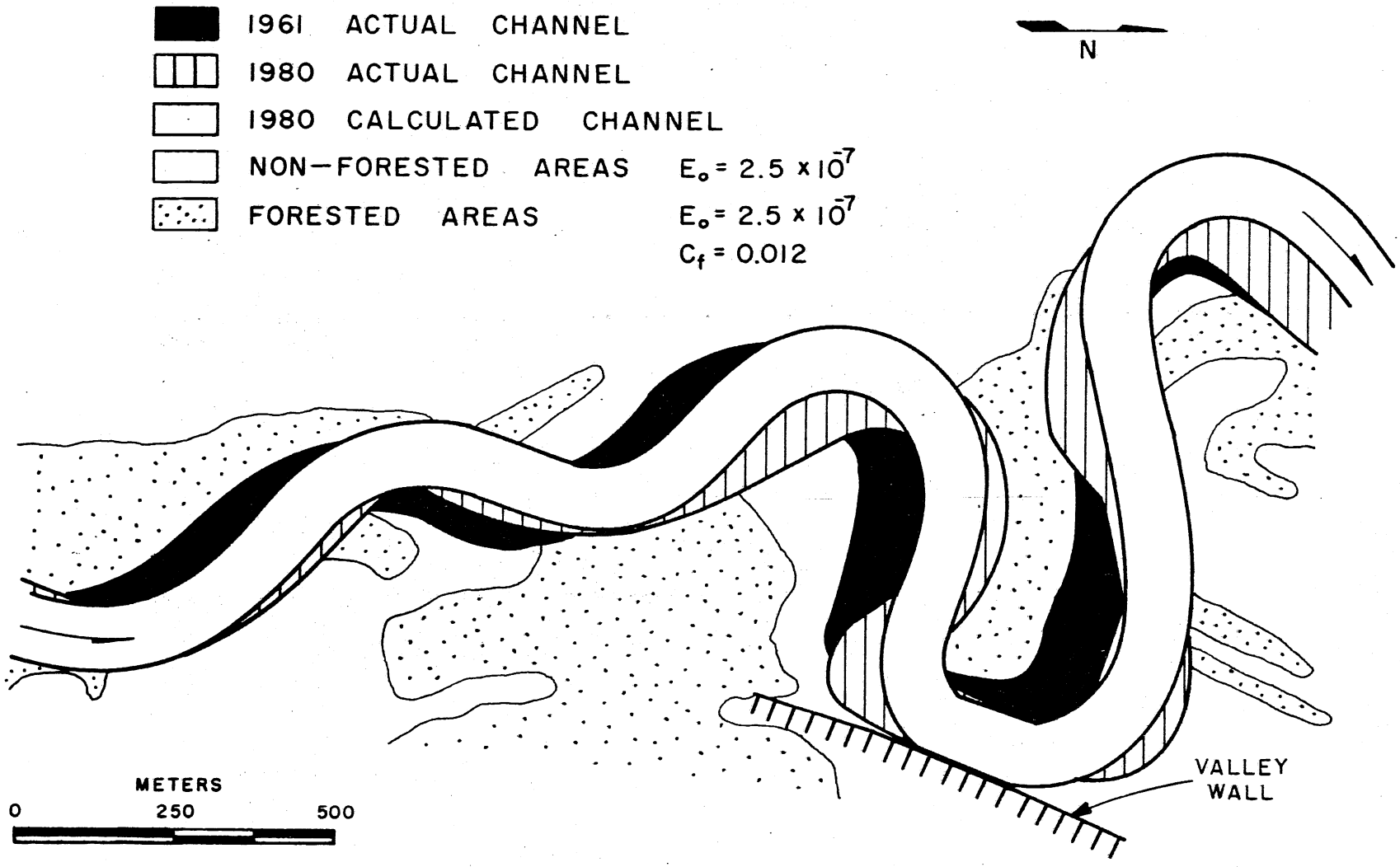

Fig. IV.23. Calibration verification, using the period between 1961 - 1980.

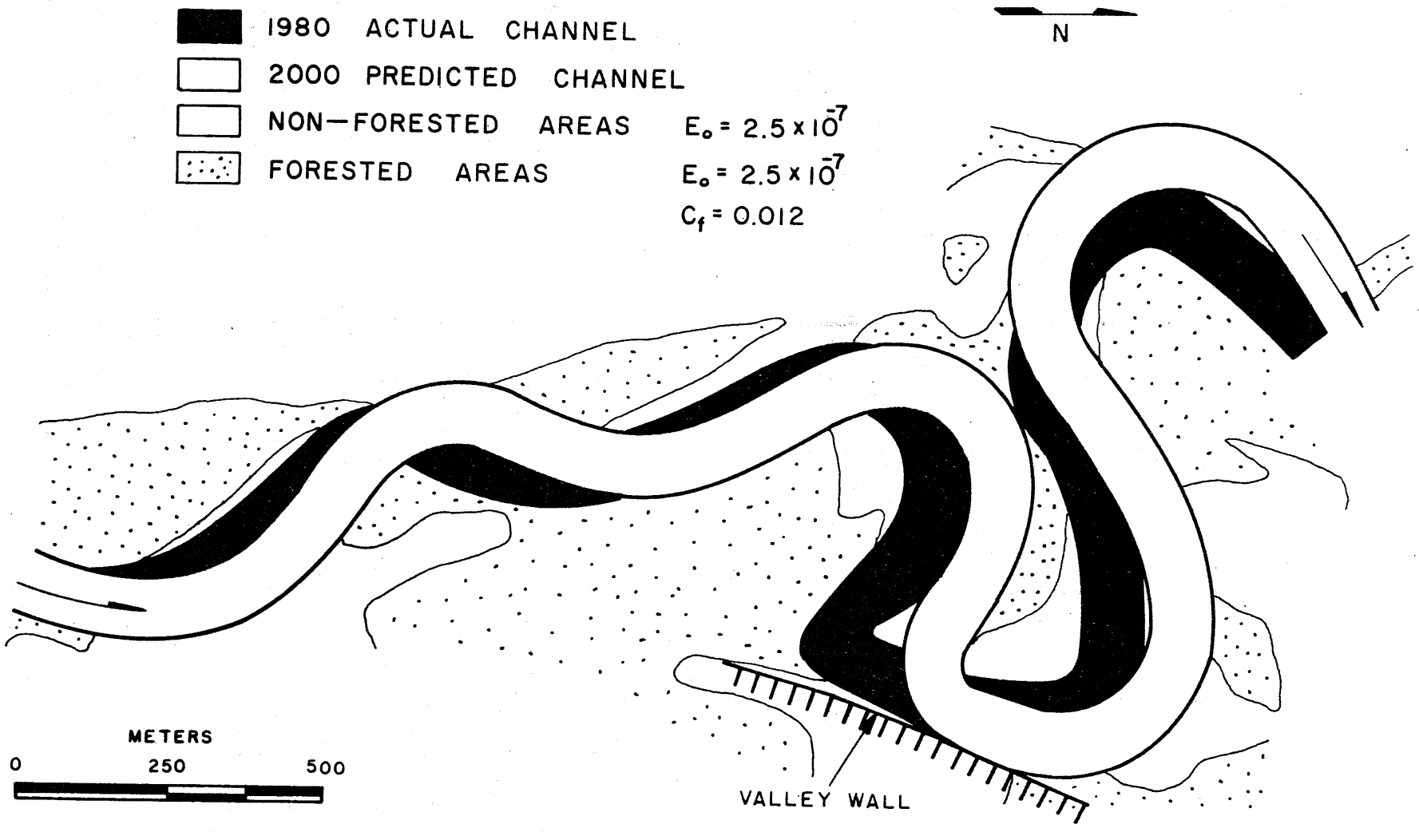

Fig.IV.24. Prediction from 1980 - 2000.

patterns of the river (Fig. IV.28). The valley has a bottom width that varies significantly and is incised approximately 11 m below the surrounding plains. It is filled with clayey silt and sand.

Channel planform. From 1939 to 1977, the sinuosity of the river changed very little within the study area and was about 1.5 to 1.6. The river flows alternately through forested and non-forested areas. Throughout the period of record, the amount and location of non-forested areas along the river banks has changed. In 1939, non-forested areas were located along the river banks for about 58% of the length of the reach. In 1954 and 1979, the corresponding values were 71% and 55%.

The valley walls restrict the migration of the river in several places (Fig. IV.28). Although they are not inerodible, the valley walls slow down the erosion so much that they can be assumed to be inerodible within the period of interest (1939-2000).

Hydrology. The Red Lake River is not gaged within the length of the study reach. However, inferences as to hydrologic conditions could be made from the gaging station at Crookston (Fig. IV.25). This gaging station has been in operation since 1901. The difference in discharge between the study reach and Crookston was assumed to be negligible due to the lack of substantial tributaries in between. Data for various flood flows are listed in Table 11; the information was compiled by the U.S. Geological Survey.

A rating curve was obtained for the gage site at Crookston. This, together with cross-section data obtained between the study reach and the gaging station, allowed for an estimation of bankfull flow in the study reach.

Channel geometry. Several cross-sections just downstream of the study reach were surveyed between 1970 and 1975 by the St. Paul District of the U.S. Army Corps of Engineers. Locations of these cross-sections are shown in Fig. IV.26. Some typical cross-sections are shown in Fig. IV.27, and cross-section characteristics are listed in Table 12. These measurements, together with a topographical map, allowed for estimation of average bankfull geometry and flow parameters, as shown in Table 13. Since the valley is very irregular, the valley slope could not be assumed to be constant over a long distance. Therefore, the influence of the difference in sinuosity between the study reach (sinuosity = 1.48) and the reach where cross-sections were surveyed (sinuosity = 1.92) could not be taken into account. Fortunately, the influence of this sinuosity difference is small. Bankfull geometry and flow parameters that would result if the river were straight, $S_i = 1$, were computed for the study reach with an assumed value for sinuosity of 1.48. These parameters were used as input data in the program, and are listed in Table 13.

2. History of Channel Planform

Aerial photographs of the channel for the years 1939, 1948, 1954, 1966, 1977, and a topographical map based on aerial photographs from 1977 were obtained. The topographical map and the aerial photographs from 1939, 1954, and 1977 were enlarged to a common scale. In Fig. IV.28, the 1939,

TABLE 11. VARIOUS FLOOD FLOWS FOR THE RED LAKE RIVER

Flow	Discharge at Crookston (m^3/s)
bankfull	330
2-year	210
5-year	380
10-year	500
25-year	660
50-year	780
100-year	890
largest on record	804

TABLE 12. CROSS-SECTION CHARACTERISTICS

Cross-section Number	Top Width (m)	Mean Depth (m)
36	131	2.7
37	107	1.9
39	61	3.3
40	81	2.9
41	62	2.1
42	75	3.8
43	--	--- (Not typical)

TABLE 13. AVERAGE PARAMETERS AT BANKFULL FLOW

	River Channel	Straight Channel
Water surface slope	$I = 3.59 \cdot 10^{-4}$	$I_o = 5.32 \cdot 10^{-4}$
Channel width	$B = 86.1$ m	$B_o = 86.1$ m
Mean depth	$H = 2.78$ m	$H_o = 2.45$ m
Discharge	$Q = 330$ m^3/s	$Q_o = 330$ m^3/s
Mean flow velocity	$U = 1.36$ m/s	$U_o = 1.55$ m/s
Froude number	$F = 0.26$	$F_o = 0.32$

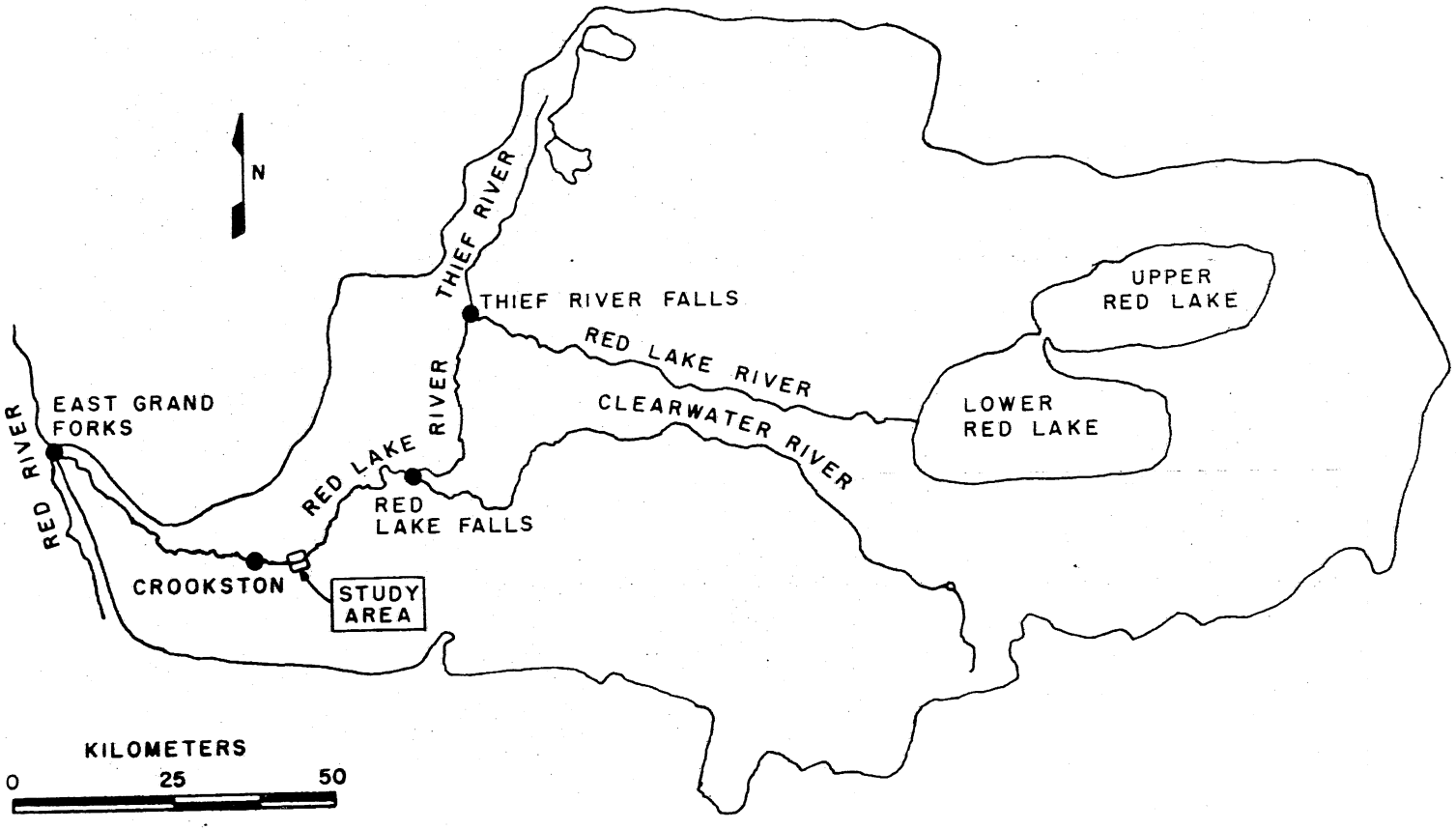

Fig. IV.25. The Red Lake River watershed.

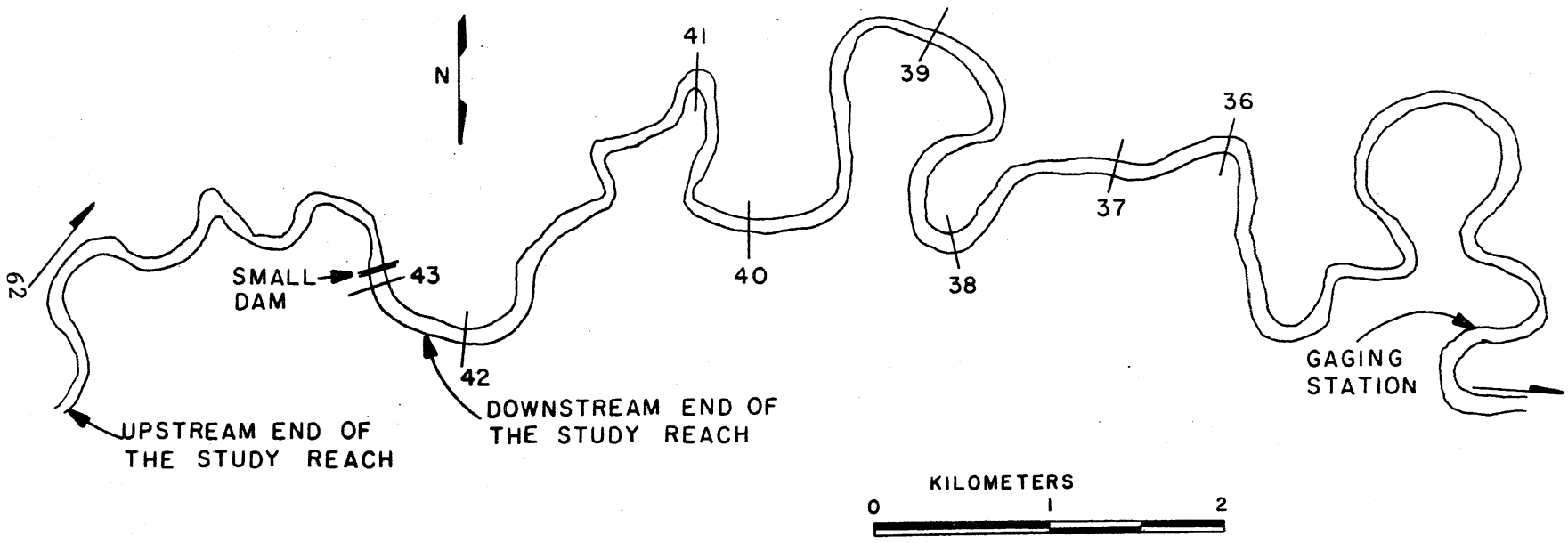

Fig. IV.26. Locations of cross-sections.

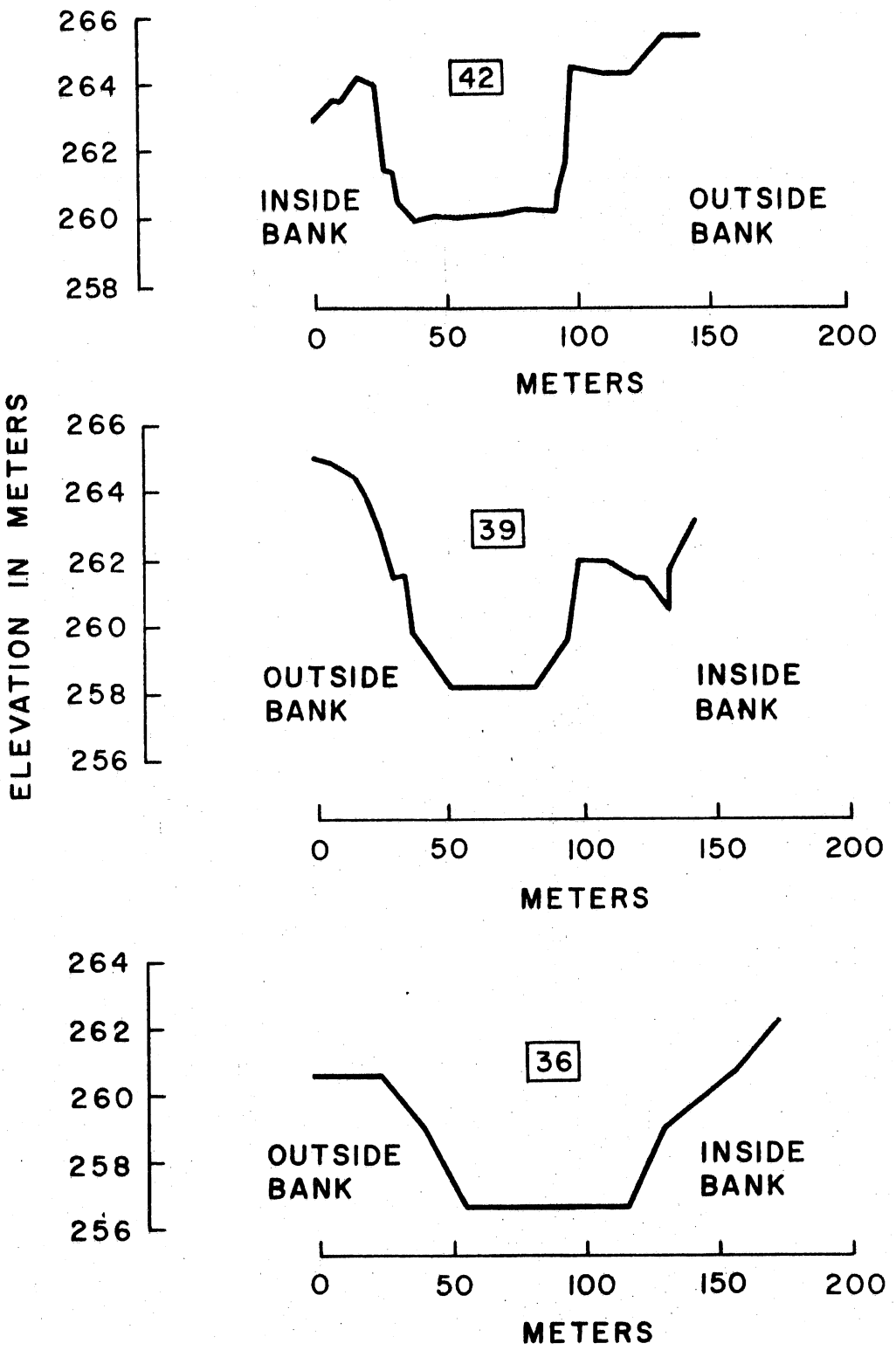

Fig. IV.27. Some typical cross-sections.

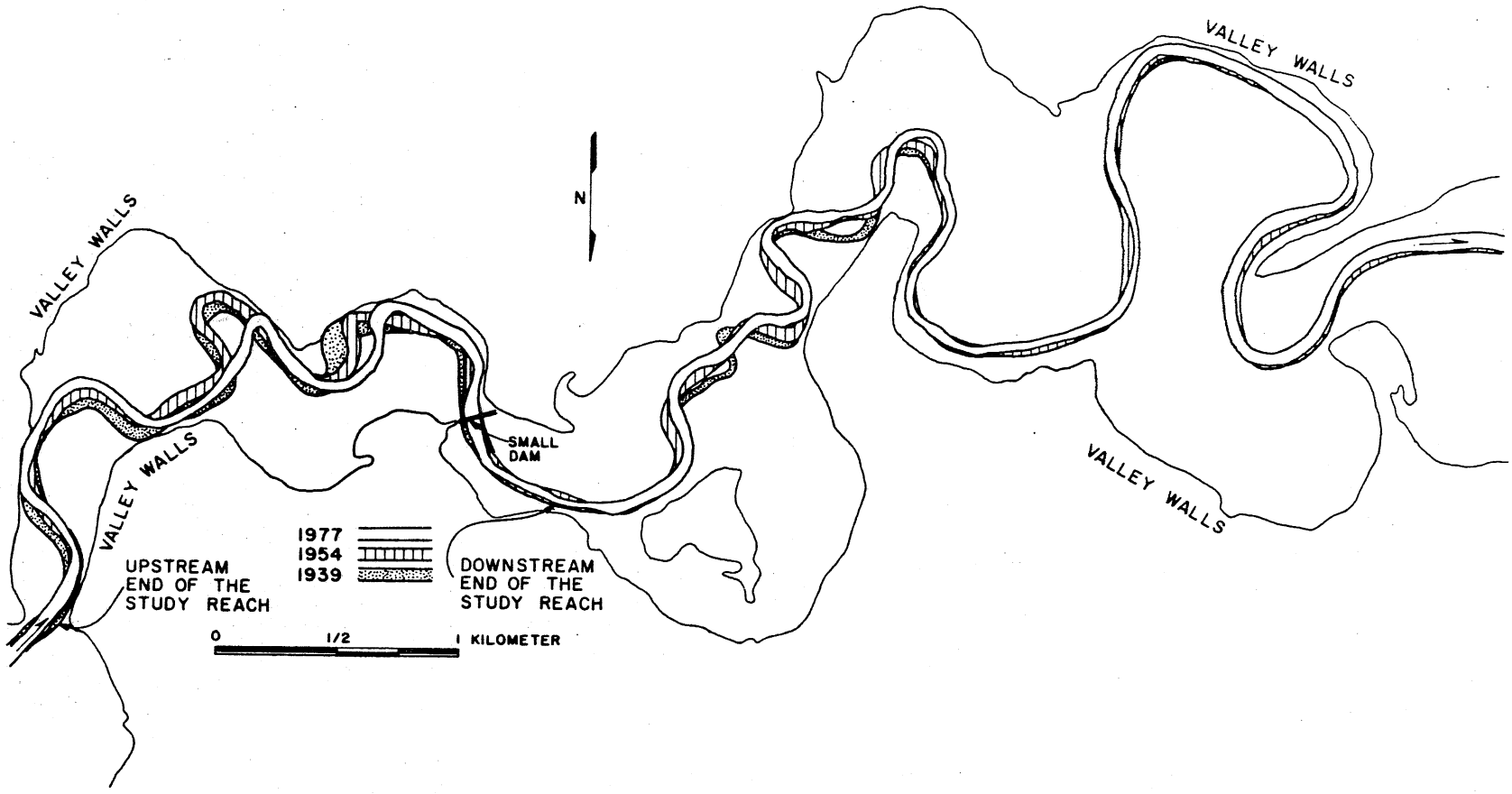

Fig. IV.28. The 1939, 1954, and 1977 channels of the Red Lake River.

1954, and 1977 channels are shown. It can be seen how the valley walls restrict the migration of the river. Within the study reach and close to the downstream end of it, there is a small dam that started to break down a few years ago (Fig. IV.28). It was assumed that the existence of the dam did not influence the meandering behavior of the river except in the immediate vicinity of the dam, where the lateral movement of the river was restricted.

3. Computer Analysis

The model was calibrated by optimizing the erosion coefficient, E_o , and the dimensionless friction factor, C_f . The period between 1954 and 1977 was used for the calibration and following values were obtained:

Non-forested areas $E_o = 1.5 \cdot 10^{-7}$

Forested areas $E_o = 5.0 \cdot 10^{-8}$

$C_f = 0.0090$

The results of this calibration are shown in Fig. IV.29. Forested and non-forested areas in that period are also indicated. The prediction of the model is seen to be very good. One reason for the excellent agreement between the predicted and the actual channel in 1977 is that the movement of the river is very restricted by the valley walls.

In order to check the calibration, the same set of values for E_o and C_f was used to calculate the movement of the river from 1939 to 1954. The results are shown in Fig. IV.30. The prediction of the model is seen to be satisfactory, although it is not as good as the agreement between the calculated and the actual channel in 1977.

Finally, the model was used to predict the location of the channel in 2000. The same set of values for E_o and C_f was used. The results are shown in Fig. IV.31.

F. Summary and Discussion of Results

1. Summary of Results

Based on the computer analysis of these four rivers, it is concluded that the model is able to reproduce past river migration reasonably well. The model, however, needs considerable calibration. It is, therefore, possible to use the model to predict the future migration of a certain river only if maps and aerial photographs are available that allow for the calibration of the model.

In Table 14, the results of the model calibration are summarized. It can be seen that the calibrated values for C_f are always considerably higher than the observed values. In Table 15, results of model calibration from previous studies are listed.

Values of the erosion coefficient, E_o , vary from $1.8 \cdot 10^{-8}$ to $2.5 \cdot 10^{-7}$ in the present study and are about two times higher for non-forested areas

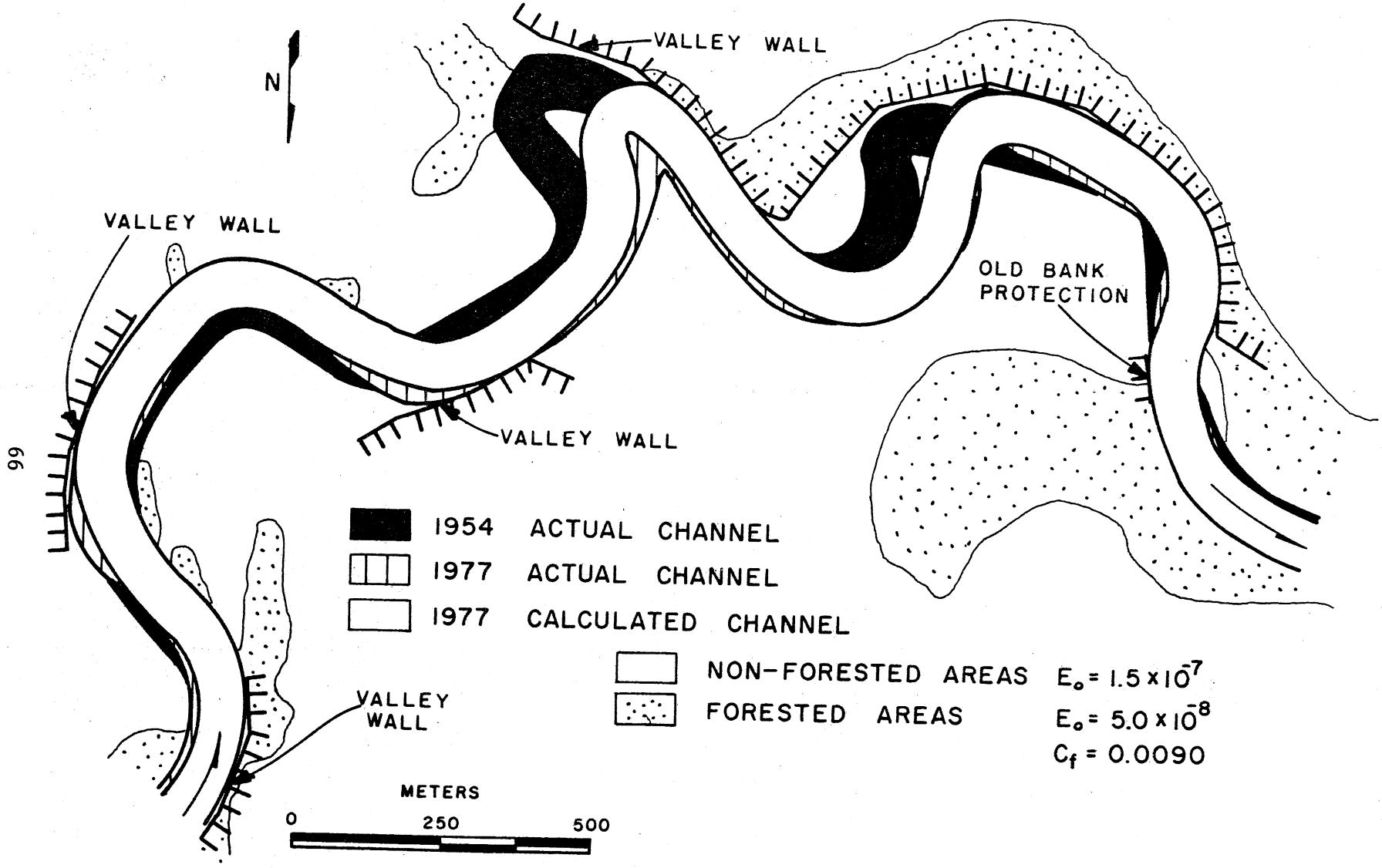

Fig. IV.29. Model calibration, using the period between 1954 - 1977.

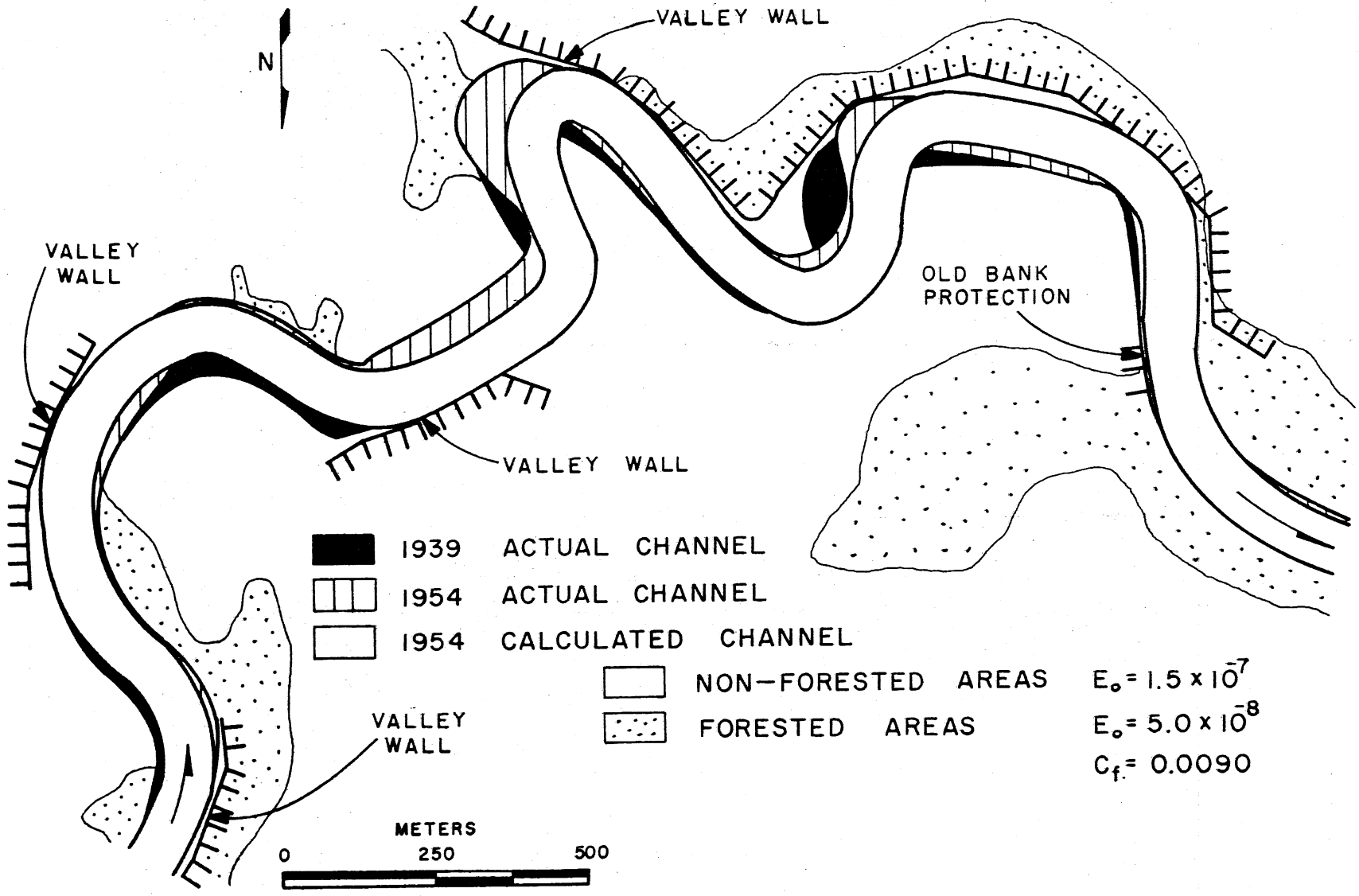

Fig. IV.30. Calibration verification, using the period between 1939 - 1954.

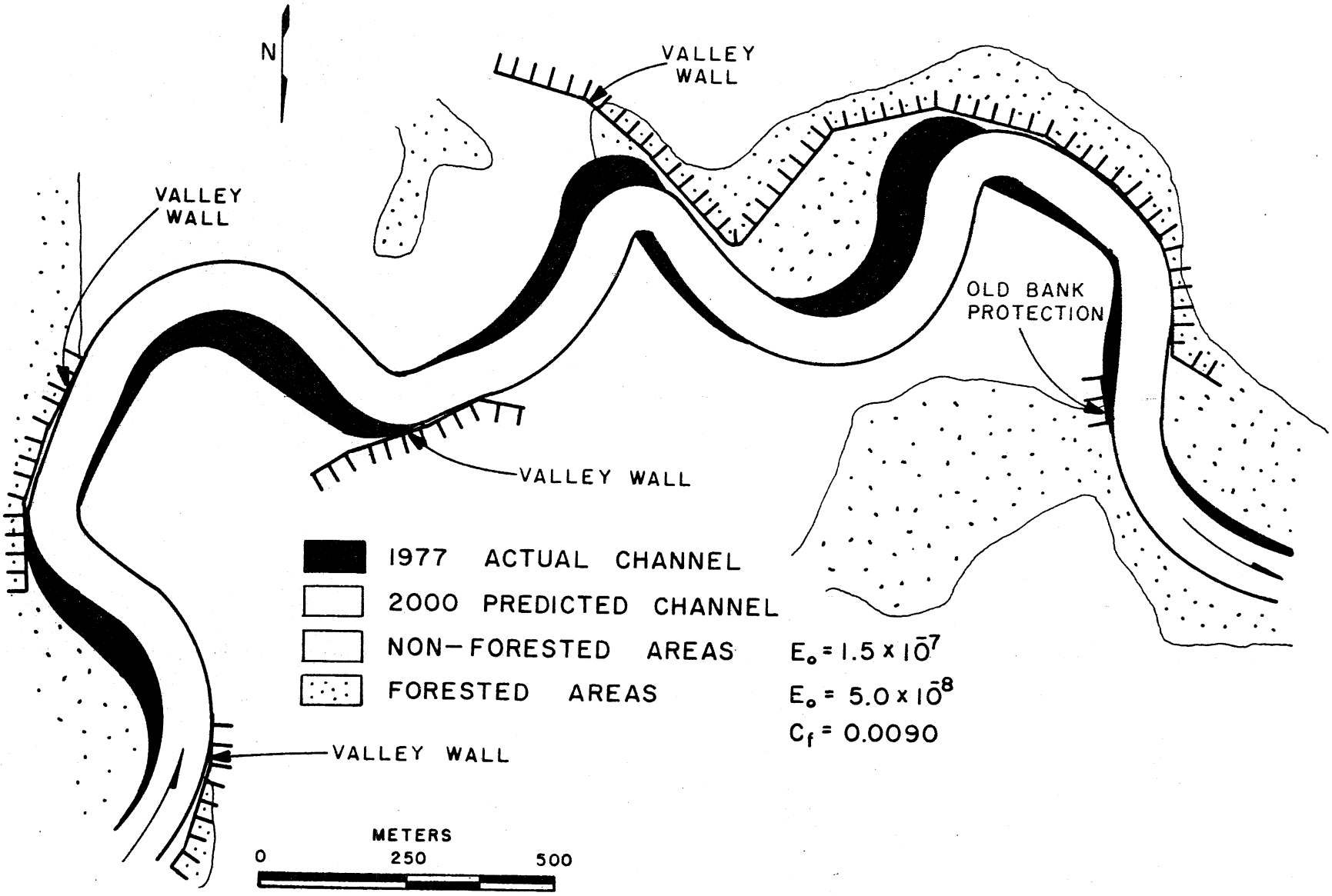

Fig. IV.31. Prediction from 1977 - 2000.

TABLE 14. RESULTS OF MODEL CALIBRATION (PRESENT STUDY)

River Name	Reach Location	C_f Calibrated	C_f Observed	$\frac{(C_f)_{cal}}{(C_f)_{obs}}$	E_o Forested Areas	E_o Non-forested Areas	$\frac{(E_o)_{Non\text{-}forested}}{(E_o)_{Forested}}$
Root River	Near Rushford	0.013	0.0021	6.2	$6.0 \cdot 10^{-8}$	$1.1 \cdot 10^{-7}$	1.8
Zumbro River	Near Kellogg	0.020	0.0042	4.8	$2.5 \cdot 10^{-8}$	$7.0 \cdot 10^{-8}$	2.7
					$1.8 \cdot 10^{-8}$	$4.9 \cdot 10^{-8}$	
Minnesota River	Near Mankato	0.012	0.0057	2.1	$2.5 \cdot 10^{-7}$	$2.5 \cdot 10^{-7}$	1.0
Red Lake River	Near Crookston	0.0090	0.0053	1.7	$5.0 \cdot 10^{-8}$	$1.5 \cdot 10^{-7}$	3.0

TABLE 15. RESULTS OF MODEL CALIBRATION (PREVIOUS STUDIES)

River Name	Reach Location	C_f Calibrated	C_f Observed	E_o Forested Areas	E_o Non-forested Areas	A
Minnesota River	Near Le Sueur, Minnesota, U.S.A.	0.012	0.0023	Same value assumed $8.0 \cdot 10^{-8}$		15.0 (assumed)
Pembina River	Near Rossington, Alberta, Canada	C_f was not calibrated	0.0067	Same value assumed $(1.5 - 3.5) \cdot 10^{-7}$		5.2 (measured)
Genesee River	Near Mount Morris, New York, Canada	C_f was not calibrated	0.0077	$3.5 \cdot 10^{-6}$	$8.0 \cdot 10^{-6}$	9.0 (calibrated)

than for forested areas. They are in line with values previously obtained by Parker [1982] for the Minnesota River and Beck et al. [1983a] for the Pembina River, Table 15. Beck et al. [1983b] obtained much higher values for the erosion coefficient when studying the Genesee River, due to the fact that constant flow rate, equal to the bankfull flow rate, was not assumed. They used the flow-duration curve to account for the time integrated effect of the entire range of flows. This obviously results in much higher values for E_o since high flow rates only occur for a relatively small percentage of the time. Their results for E_o are thus not comparable with the present study.

Parker [1982] set the value of A equal to 15 for the Minnesota River. This corresponds to a value of A = 16 in the modified computer model, as noted in Chapter II.B.2. The resulting calibrated value for C_f was 5.2 times higher than the observed value. This result shows the same trend as the result from the present study. It is interesting that the calibrated value of C_f was this high. If the selected value of A would be reduced, the calibrated value of C_f would become still higher, as can be seen from Eqs. (15) and (19). It is also worth noting that the accuracy of the input parameters used by Parker [1982] is higher than the accuracy of the input parameters used in the present study since cross-sections were surveyed within the study reach.

Beck et al. [1983a] set the value of A equal to 5.2 when analyzing the Pembina River. This corresponds to a value of A = 6.2 in the modified computer model. The value of A was based on rather extensive cross-section measurements. The model was calibrated by only varying the value of the erosion coefficient, E_o , and the result was satisfactory.

Beck et al. [1983b] calibrated the model by varying the values of E_o and A when analysing the Genesee River. The calibrated value of A was equal to 9.0, which corresponds to a value of A = 10 in the modified computer model. The result was rather good.

As can be seen from the above discussion, there are several different ways in which the model can be calibrated. However, the only method that always gives satisfactory results is to set the value of A equal to the measured value or equal to about six if measurements are not available. Then the model is calibrated by varying the values of E_o and C_f. This procedure was used successfully herein.

2. Discussion

The consistent result of higher calibrated than observed values of the dimensionless friction factor, C_f , merits further discussion. The influence of increasing the value of C_f is shown in Fig. IV.3a. It shifts the velocity distribution upstream, thus making the velocity higher at the outside bank than the inside bank at the bend apex. This results in the classical meandering pattern of outward growing and downstream shifting bends. If the observed value of C_f was used, the bends generally decreased in amplitude as they migrated downstream. Several reasons may account for this lack of the model capability to predict satisfactory migration pattern using the observed value of C_f. When discussing these reasons, it is important to remember that the theory consists of two independent parts.

They are the flow field model, the result of which is given by Eq. (15), and the bank erosion model consisting of Eqs. (23) and (24a,b). The solution for the flow field is used as input data for the bank erosion model. Any lack of performance of the model can therfore either be caused by errors in the flow field, or if the flow field is satisfactory, then in the bank erosion model.

There are several reasons why the flow field model may predict that the high-velocity core shifts from the inside bank to the outside bank downstream of the bend apex leading to decreasing bend amplitude.

1) Since the momentum equations used herein are depth-averaged, the influence of the secondary currents has been partially lost (the influence of the secondary currents on the sediment transport is to some extent accounted for by introducing the tranverse bed slope parameter A). This results in decreased velocity at the outside bank in a bend, since secondary currents transport high momentum fluid from the inside bank to the outside bank and low momentum fluid from the outside bank to the inside bank. This is discussed by Kalkwijk & DeVriend [1980].

2) The assumption that the bed topography is a function of the local curvature is not always a very good one, as discussed by Struiksma et al. [1985]. They obtained the result that a significant part of the lateral bed slope is induced by the redistribution of water and sediment motion in the first part of the bend. However, it is difficult to say if this leads to increased or decreased velocity at the outside part in a bend, since the value of the transverse bed slope parameter, A, was not theoretically calculated herein.

3) Dietrich & Smith [1983] and Smith & McLean [1984] emphasized the the role of the convective acceleration terms in Eqs. (1a,b), some of which are neglected herein. Smith & McLean [1984] developed a computer model that used Engelund's second approximation to simplify Eq. (1b), and then used an iteration procedure to solve Eq. (1a) for the downstream velocity component, without dropping any terms. They then used this result to get a higher order estimate for the transverse velocity component from Eq. (1b). It is possible that this more accurate calculation of the flow field will give a solution that shifts the high-velocity core towards the outside bank of a bend earlier than in the current solution.

Finally, it is quite possible that the current model is giving a satisfactory solution for the flow field, and that the main error is introduced by the bank erosion model. The bank erosion model assumes a direct relationship between the bank erosion rate, $\tilde{\zeta}$, and the velocity perturbation, u'_b , as given by Eq. (23). Inherent in this relationship is the assumption that river migration is due to erosive removal of soil particles, from the bank, by streamflow. However, it has been observed in the field that most of the river migration is often caused by failure of a saturated bank following a rapid drop in water level. This indicates that the bank erosion rate might be a function of both the velocity perturbation,

u'_b, and the flow depth perturbation, h'_b, where $h'_b = h'$ at $\tilde{n} = b$. This can be explained as follows: Erosion of the bank toe due to streamflow steepens the bank and thus faciliates the failure of a saturated bank. Secondly, as the bank is higher, (the variation in bank height from the mean is equal to h'_b), it is more likely to fail. An improved bank erosion model could therefore possibly be obtained through the following relationship

$$\tilde{\zeta} = E_o\left(u'(\tilde{s},b) + \beta h'(\tilde{s},b)\right) \tag{38}$$

where β is a positive constant, which would be obtained by calibration. Hopefully, it would not vary too much between different rivers. It is obvious that this additional term in the bank erosion model will always increase the outward growth rate of a bend, since according to the present model, $h'(\tilde{s},b)$ is always positive at the outside bank in a bend and always negative at the inside bank, as can be seen from below.

$$h'(\tilde{s},b) = (\xi' - \eta')_{\tilde{n}=b} \approx -\eta' = AC'bH \tag{39}$$

Based on the above discussion, it is concluded that there are several different ways in which the computer model used herein may be improved. The recommended approach is to compare the computed flow field to field data or experimental results available in the literature. If satisfactory agreement is obtained between the calculated and the measured flow field, the emphasis should be shifted toward the bank erosion model, possibly trying the approach given by Eq. (38). However, if the agreement between the calculated and the measured flow field is not satisfactory, the flow field model must be improved before the bank erosion model is changed, since there is no easy way to test the bank erosion model.

V. SUMMARY AND CONCLUSIONS

A. Summary

This study was aimed primarily at evaluating the overall performance of an already-existing computer model for simulation of the migration of meandering rivers.

In Chapter II, the theory behind the computer model is derived. It differs slightly from the derivation by Ikeda et al. [1981]. It is shown that for a flat bed channel, i.e. $A = 0$, bends will not grow in amplitude unless the flow is supercritical. This differs from the result obtained by Ikeda et al. [1981] that a flat bed channel could be unstable for certain combinations of C^*_{f1} and F although the flow is not supercritical.

In Chapter III, a brief description is given of the computer model.

In Chapter IV, the computer model is applied to four rivers in the state of Minnesota. A general procedure for use of the model is given. A detailed explanation of how the input parameters were estimated is also provided. The results of the calibration and the verification of the model are given in the form of graphs, which show both the initial locations and the measured and calculated final locations of the rivers. The model was also used to predict the future locations of these rivers in the year 2000. Finally, the results are summarized and the conclusion drawn that the theoretical basis of the model is somewhat insufficient, since the calibrated values of C_f were always higher than the observed values. Some possible reasons for this are listed, and an outline is given for future research that hopefully will improve the modelling theory.

B. Conclusions

Based on the results obtained by applying the computer model to four rivers, it is concluded that the model is able to reproduce past river migration reasonably well. However, it needs considerable calibration. It is therefore possible to use this model to predict future migration of a certain river only if maps and aerial photographs are available that allow for the calibration of the model.

It was found that the rivers typically eroded about two times faster through non-forested areas than through forested areas. This result is of some interest, especially in agricultural areas. It indicates the importance of having a grove of trees lining the river instead of farming all the way to the river bank.

The consistent result of calibrated values for the dimensionless friction factor, C_f, that are higher than observed, indicates that the modelling theory needs to be improved. The recommended approach is to compare the computed flow field to field data or experimental results

available in the literature. If satisfactory agreement is obtained between the calculated and the measured flow field, the emphasis should be shifted toward the bank erosion model, possibly trying the approach given by Eq. (38). However, if the agreement between the calculated and the measured flow field is not satisfactory, the flow field model must be improved before the bank erosion model is changed, since there is no easy way to test the bank erosion model.

BIBLIOGRAPHY

Adachi, S. 1967. A theory of stability of streams. Proc. 12th Congr. IAHR, Vol. 1, pp. 338-343.

Beck, S. M. 1985a. Computer simulated deformation of meandering patterns. Ph.D. thesis, Univ. of Minnesota.

Beck, S. M. 1985b. Self stabilization of stalled meander bends. Canadian Society for Civil Eng., Annual Conference, May, 27-31,1985, Saskatoon, Saskatchewan, Canada.

Beck, S. M, Harrington, R. A. & Andres, D. D. 1983a. Lateral channel stability of the Pembina River near Rossington, Alberta. Alberta Research Council Report, Edmonton, Alberta.

Beck, S., Melfi, D. A. & Yalamanchili, K. 1983b. Lateral migration of the Genesee River, New York. Proc., Rivers '83 Speciality Conference on River Meandering, ASCE, Oct., 24-26, 1983, New Orleans, U.S.A.

Blondeaux, P. & Seminara, G. 1985. A unified bar-bend theory of river meanders. (In press, Journal of Fluid Mechanics).

Callander, R. A. 1969. Instability and river channels. Journal of Fluid Mechanics, Vol. 36, pp. 365-480.

Dietrich, W. E. & Smith, J. D. 1983. Influence of the point bar on flow through curved channels. Water Resources Research, American Geophysical Union, Vol. 19, No. 5, pp. 1173-1192.

Dietrich, W. E. & Smith, J. D. 1984. Bed load transport in river meander. Water Resources Research, Vol. 20, No. 10, pp. 1355-1380.

Engelund, F. 1974. Flow and bed topography in channel bends. ASCE Journal of the Hydraulics Division, Vol. 100, No. HY11, pp. 1631-1648.

Engelund, F. & Skovgaard, O. 1973. On the origin of meandering and braiding in alluvial streams. Journal of Fluid Mechanics, Vol. 57, pp. 289-302.

Fredsoe, J. 1978. Meandering and braiding of rivers. Journal of Fluid Mechanics, Vol. 84, pp. 607-624.

Guetzkow, L. C. 1977. Techniques for estimating magnitude and frequancy of floods in Minnesota. U.S. Geologocal Survey, Water Resources Investigations Report No. 77-31.

Hansen, E. 1967. The formation of meanders as a stability problem. Hydraul. Lab., Tech. Univ. of Denmark, Basic Res. Prog. Rep., No. 13.

Hayashi, T. 1970. The formation of meanders in rivers. Proc. Japan Soc. Civ. Eng., No. 180 (in Japanese).

Hayashi, T. & Ozaki, Y. 1976. On the meander wavelength from the view point of bar instability theory. Proc. 20th Annual Meeting, Hydraul., Japan Soc. Civ. Eng., pp. 89-96 (in Japanese).

Henderson, J. E., Shields, F. D. 1984. Enviromental features for streambank protection projects. U.S. Army Engineer Waterways Experimental Station, Technical Report E-84-11.

Hickin, E. J. 1974. The development of meanders in natural river channels. American Journal of Science, Vol. 274, pp. 414-442.

Hickin, E. J. 1978. Mean flow structure in meanders of the Squamish River, British Columbia. Canadian Journal of Earth Sciences, Vol. 15, pp. 1833-1849.

Hickin, E. J. & Nanson, G. C. 1975. The character of channel migration of the Beatton River, Northeast British Columbia, Canada. Geological Society of America Bulletin, Vol. 86, pp. 487-494.

Hooke, R. L. 1975. Distribution of sediment transport and shear stress in a meander bend. Journal of Geology, Vol. 83, Sept., pp. 543-565.

Howard, A. D. 1983. Simulation model of meandering. Proc., Rivers '83 Speciality Conference on River Meandering, ASCE, Oct., 24-26, 1983, New Orleans, U.S.A.

Ikeda, S. 1975. On secondary flow and bed profile in alluvial curved open channel. Proc. 16th Congr. IAHR, Vol. 2, pp. 105-112.

Ikeda, S., Parker, G. & Sawai, K. 1981. Bend theory of river meanders. Part 1. Linear development. Journal of Fluid Mechanics, Vol. 112, pp. 363-377.

Kalkwijk, J. P. TH. & DeVriend, H. J. 1980. Computation of the flow in shallow river bends. IAHR, Journal of Hydraulic Research, Vol. 18, No. 4, pp. 327-342.

Keown, M. P., Oswalt, N. R., Perry, E. B., Dardeau, E. A. 1977. Literature survey and preliminary evaluation of streambank protection methods. U.S. Army Engineer Waterways Experiment Station, Technical Report H-77-9.

Kikkawa, H., Ikeda, S. & Kitagawa, A. 1976. Flow and bed topography in curved open channels. ASCE, Journal of the Hydraulics Division, Vol. 102, No. HY9, pp. 1327-1342.

Nanson, G. C. & Hickin, E. J. 1983. Channel migration and incision on the Beatton River. ASCE, Journal of the Hydraulics Division, Vol. 109, No. HY3, pp. 327-337.

Odgaard, J. A. 1981. Transverse bed slope in alluvial channel bends. ASCE, Journal of the Hydraulics Division, Vol. 107, No. HY12, pp. 1677-1694.

Parker, G. 1975. Meandering of supraglacial melt streams. Water Resources Research, Vol. 11, pp. 551-552.

Parker, G. 1976. On the cause and characteristic scales of meandering and braiding in rivers. Journal of Fluid Mechanics, Vol. 76, pp. 457-480.

Parker, G. 1982. Stability of the channel of the Minnesota River near State Bridge No. 93, Minnesota. St. Anthony Falls Hydraulic Laboratory Project Report No. 205, Univ. of Minnesota, Minneapolis, Minnesota.

Parker, G. 1983. Theory of meander bend deformation. Proc., Rivers '83 Speciality Conference on River Meandering, ASCE, Oct., 24-26, 1983, New Orleans, U.S.A.

Parker, G. & Andrews, E. D. 1985. On the time development of meander bends. Manuscript submitted to the Journal of Fluid Mechanics.

Parker, G., Sawai, K. & Ikeda, S. 1982. Bend theory of river meanders. Part 2. Nonlinear deformation of finite amplitude bends. Journal of Fluid Mechanics, Vol. 115, pp. 303-314.

Parker G., Diplas, P. & Akiyama, J. 1983. Meander bends of high amplitude. ASCE, Journal of the Hydraulics Division, Vol. 109, No. 10, pp. 1323-1337.

Ponce, V. M. & Mahmood, K. 1976. Meandering thalwegs in straight alluvial channels. Proc. ASCE Rivers Conference 1976, Fort Collins, Colorado.

Rozovskii, I. L. 1957. Flow of water in bends of open channels. Academy of Sciences of U.S.S.R. Translated by Y. Prushanski, the Israel Program for Scientific Translations, 1961.

Smith, J. D. & McLean, S. R. 1984. A model for flow in meandering streams. Water Resources Research, Vol. 20, No. 9, pp. 1301-1315.

Struiksma, N., Olesen K. W., Flokstra, C., Vriend, H. J. HE. 1985. Bed deformation in curved alluvial channels. IAHR, Journal of Hydraulic Research, Vol. 23, No. 1, pp. 57-79.

Suga, K. 1963. On local scour at river bends. Tech. Memo Public Works Res. Inst., Min. of Const. Japan, Vol. 5, No. 4 (in Japanese).

Sukegawa, N. 1970. Conditions for the occurrence of river meanders. Journal of the Faculty of Engineering., Univ. of Tokyo, Vol. 30, pp. 289-306.

Tamai, N. & Ikeuchi, K. 1984. Longitudinal and transverse variations of the depth-averaged flow fields in a meandering channel. Journal of Hydroscience and Hydraulic Engineering, Vol. 2, No. 2, pp. 11-33.

Zimmerman, C. & Kennedy, J. F. 1978. Transverse bed slopes in curved alluvial streams. ASCE, Journal of the Hydraulics Division, Vol. 104, No. HY1, pp. 33-48.

APPENDIX: STREAMBANK PROTECTION METHODS

A.1 Introduction

Since streambank protection is commonly used to slow down or stop river migration, it was considered appropriate to include herein an overview of available bank protection methods.

A.2 Types of Streambank Erosion

The most common types of streambank erosion are:

a) Attack at the toe of the underwater slope, leading to bank failure and erosion. This type of bank failure commonly follows a rapid drop in water level.

b) Erosion of soil along the bank caused by current action.

c) Sloughing of saturated cohesive banks, i.e. banks incapable of free drainage, due to rapid drawdown.

d) Flow slides (liquefaction) in saturated silty and sandy soil.

e) Erosion of the soil by seepage out of the bank at relatively low channel velocities.

f) Erosion of upper bank, river bottom or both due to wave action caused by wind or passing boats.

A.3 Streambank Protection Methods

Streambank protection methods can be classified as direct or indirect.

1) Direct methods: These involve placing materials such as stone, fabrics or vegetation in contact with the bank to shield it from erosive forces. Example:

    a) Riprap revetment
    b) Concrete pavement
    c) Articulated mattresses made of concrete block and wire
    d) Asphalt
    e) Erosion-control fabrics and mats
    f) Vegetation
    g) Used-tire matting
    h) Gabions

2) Indirect methods: Involve use of structure to deflect erosive currents away from the bank and reduce velocities next to the bank.

    a) Transverse dikes
    b) Fences
    c) Jacks

An attempt will not be made to describe each of these methods nor will any selection or design criteria be given. However, it is worth mentioning that if stones of sufficient size are available, riprap is usually the first choice among the bank protection methods considered because of the following general advantages:

a) A riprap blanket is flexible and is neither impaired nor weakened by slight movement of the bank resulting from settlement or other minor adjustments.

b) Local damage or loss is easily repaired by the placement of more rock.

c) Construction is not complicated and no special equipment or construction practices are necessary.

d) Appearance is natural, hence acceptable in recreational areas.

e) If riprap is exposed to fresh water, vegetation will often grow through the rocks adding structural value to the bank material and restoring natural roughness.

f) Riprap is recoverable and may be stockpiled for future use.

Meeting the design objectives necessary to guarantee effective bank protection by riprap blanket requires:

a) Determination of the shape, size and weight of the stones in the riprap blanket that will be stable under excessive hydraulic conditions.

b) Well-graded bedding material or filter cloth that will prevent erosion of the bank material through the blanket.

c) Optimum riprap blanket and bedding material thickness.

d) Proper termination of the riprap blanket.

A more detailed description of all the above-mentioned bank protection methods is given by Keown et al. [1977] and Henderson et al. [1984].